INSTITUTO SUPERIOR DE ENGENHARIA DE LISBOA

Área Departamental de Engenharia de Electrónica e Telecomunicações e de Computadores

MIMO Antenna for Mobile Terminal

Paulo Roque Simões Capitão

Licenciado

Dissertação para obtenção do Grau de Mestre
em Engenharia Eletrónica de Telecomunicações e de Computadores

Orientadores : Prof. Doutor Pedro Pinho
Prof. Doutor Carlos Mendes

Júri:

Presidente: Prof. Nuno Cota

Vogais: Prof. Doutor Henrique Salgado
Prof. Doutor Pedro Pinho

março, 2021

INSTITUTO SUPERIOR DE ENGENHARIA DE LISBOA

Área Departamental de Engenharia de Electrónica e Telecomunicações e de Computadores

MIMO Antenna for Mobile Terminal

Paulo Roque Simões Capitão

Licenciado

Dissertação para obtenção do Grau de Mestre
em Engenharia Eletrónica de Telecomunicações e de Computadores

Orientadores : Prof. Doutor Pedro Pinho
Prof. Doutor Carlos Mendes

Júri:

Presidente: Prof. Nuno Cota

Vogais: Prof. Doutor Henrique Salgado
Prof. Doutor Pedro Pinho

março, 2021

Acknowledgments

First and foremost I want to thank my advisors, Prof. Pedro Pinho and Prof. Carlos Mendes. They have been exemplar, in both academic and personal aspects. My special thanks go to them for all their knowledge and the motivation they gave me, the critics, the praises, their professionalism and dedication. I could not have done it without their help and support.

I would also like to thank the Instituto de Telecomunicações de Aveiro, for providing material and equipment for the fabrication and measurement of the antennas developed in this work.

To my parents, for all their support, incentive, patience and advises. Through all my academic journey, the good and bad moments, they were always there and believed in me, no matter what. No words can express my eternal gratitude.

A very special thanks to my sister Alexandra and to my friend Reys for all the encouragement and interest on the progress of this thesis. They were there every step of the way.

Thank you my friends André, Gonçalo, David, Tiago and Pedro for all the friendship and fellowship demonstrated throughout our academic course. Their help and presence along the road will never be forgotten.

Last but not least, to those who are not mentioned here that directly or indirectly contributed, in some way, to my journey so far.

Abstract

Nowadays there is a great demand for quality of service, higher bit rate and greater efficiency in mobile terminals, leading to technological advances in the world of telecommunications. MIMO technology makes use of multiple antennas in transmission and reception, allowing a higher data transfer rate and greater reliability without the need for extra power and bandwidth.

In this MSc dissertation a planar IFA antenna was designed, which operates in the 2 Wi-Fi frequency bands of 2.4 GHz and 5 GHz. A MIMO system with 4 antennas based on the planar IFA, and its performance is analysed through key parameters such as correlation between elements, diversity gain and multiplexing efficiency. After the simulation and analysis of the system, a prototype was fabricated and measured in order to validate the coverage of the designated frequencies.

The results achieved show that the designed antenna is feasible for WiFi applications, covering the intended frequency bands. In simulation the antenna obtains a good performance in terms of MIMO parameters. A size/performance trade-off was applied to the final design, in favour of decreasing the size of the structure to make it possible to use it in smaller size devices.

Keywords: MIMO, antenna, correlation, diversity gain, multiplexing efficiency

Resumo

Nos dias de hoje existe uma maior exigência de qualidade de serviço, maior débito binário e maior eficiência nos terminais móveis, levando ao avanço tecnológico do mundo das telecomunicações. A tecnologia MIMO faz uso de múltiplas antenas na transmissão e na recepção, permitindo uma maior taxa de transferência de dados e uma maior fiabilidade sem a necessidade de aumentar a potência e largura de banda extra.

Nesta dissertação de mestrado foi dimensionada uma antena IFA planar, que atua nas 2 bandas de frequência Wi-Fi de 2.4 GHz e 5 GHz. Um sistema MIMO com 4 antenas baseado nesta antena é concebido, sendo o seu desempenho analisado através de parâmetros chave, como a correlação entre elementos, ganho de diversidade e a eficiência de multiplexagem. Após a simulação e análise do sistema, foi fabricado e medido um protótipo de forma a validar o desempenho da antena projetada.

Os resultados alcançados demonstram que a antena projetada é viável para aplicações WiFi, cobrindo as bandas de frequência pretendidas. Em simulação a antena obtém um bom desempenho em termos de parâmetros MIMO. Foi aplicado ao design final um compromisso dimensão/desempenho, em prol de diminuir o tamanho da estrutura para tornar possível a sua utilização em dispositivos móveis de tamanho mais reduzido.

Palavras-chave: MIMO, antena, correlação, ganho de diversidade, eficiência de multiplexagem

Contents

List of Figures

List of Tables

Acronyms

AWGN	Additive White Gaussian Noise
DG	Diversity Gain
ECC	Envelope Correlation Coefficient
EGC	Equal Gain Combining
IFA	Inverted F-shaped Antenna
IoT	Internet of Things
ISM	Industrial, Scientific and Medical
LTE	Long Term Evolution
ME	Multiplexing Efficiency
MEG	Mean Effective Gain
MIMO	Multiple-Input Multiple-Output
MISO	Multiple-Input Single-Output
MRC	Maximal Ratio Combining
PCB	Printed Circuit Board
PIFA	Planar Inverted F-shaped Antenna
RF	Radio Frequency
SC	Selection Combining
SIMO	Single-Input Multiple-Output
SISO	Single-Input Single-Output
SNR	Signal to Noise Ratio
TD-LTE	Time Division - Long Term Evolution
TD-SCDMA	Time Division - Synchronous Code Division Multiple Access
TIC	Tunable Inductor and Capacitor
USB	Universal Serial Bus
Wi-Fi	Wireless Fidelity

WLAN	Wireless Local Area Network
XPR	Cross Polarization Ratio

1

Introduction

This chapter introduces the theme of this dissertation, Antenna MIMO design for mobile terminals. The motivation and objectives are presented and document's structure is given.

1.1 Framework

Over the years, the telecommunication's world has been in continuous technological growth. This led to new gadgets, apps and trends, which aim to supply the needs of the users. The increase of capacity and connectivity range are key factors when it comes to the telecommunication's evolution.

Nowadays, the mobile device is a must for anyone. Every information, every connection, every service or app can be achieved by it; The easy access to smartphones made available the acquisition by anyone, leading to a more narrowed available service bandwidth. This was compensated by the development of new technologies, including on the mobile terminal.

In the mobile terminal's development, there are elements which can be improved, like the size of it, the energy consumption, or even the processing speed. Another element that can be enhanced is the connection via radio interface, that can be accomplished by improving the mobile antenna.

The radio interface plays an important role on telecommunications. If the system is not well planned, the connection may not be established or, even if it is, the throughput may not be acceptable.

As the number of wireless clients grows, it was necessary to help lessen the bandwidth congestion, one of the methods being the use of MIMO. For wireless communication, the antennas at both sides of the wireless link and the corresponding radio propagation characteristics play an important role in the system design and optimization.

1.2 Objectives

This thesis' objectives is to design a MIMO antenna for a mobile terminal that verifies the following requirements:

- **Achieve good matching level:** S_{11} is the return loss of the antenna and one of the important parameters of antenna testing. It deals with how perfectly the input/output impedance matching is done and amount of power that is transferring to/from the antenna. If impedance matching is done perfectly then maximum power from source to antenna will be transferred. With S_{11} < -10dB 90% of power is effectively transferred to the antenna and only 10% is reflected back;
- **Support of both 2.4GHz and 5GHz ISM bands:** The first bandwidth (2.401 GHz < f < 2.48 GHz) is the radio frequency ranges used for the 2.4GHz band, by the

802.11 standard [1]. The second bandwidth (5.150 GHz< f < 5.835 GHz) is the radio frequency ranges used for the 5 GHz band, by the 802.11 standard;

- **Evaluate and optimize MIMO performance:** The use of MIMO configuration is only viable if its performance shows great improvement; this can be evaluate it by its MIMO parameters results;
- **Produce a compact antenna:** As the goal is to implement this antenna in nowadays devices, its dimensions are important and should be reduced as much as possible.

1.3 Document organization

The document is organized as follows. **Chapter 1** details the dissertation's framework, motivation and its objectives. The organization of the document is also presented. In **Chapter 2** the technology overview is presented referencing Mobile Communications Networks, MIMO Antennas, and Antenna Diversity, which are fundamental for this thesis and the state of the art as well, making use of different papers to reflect the mobile antenna's development. **Chapter 3** presents the process on the Simulation System Model, including the steps taken on the antenna design and the simulation results' analysis are presented. In **Chapter 4** the chosen design is considered for different MIMO system configurations and analysed its results, a prototype of a 4 element MIMO antenna is manufactured and measured. The **Chapter 5** summarizes the dissertation's work, the conclusions drawn and possible future improvements.

1.4 Original Contributions

With the work developed in this MSc dissertation, it was submit the following paper:

Paulo Capitão, Pedro Pinho and Carlos Mendes. A four port MIMO antenna for dual band Wi-Fi operation.

2

Technology Overview

Over the last years there has been an exponential growth in the field of wireless communication. A few years ago a user was satisfied making a call, with reasonable quality, to another mobile terminal. These days users require high-definition video on their mobile devices. Due to the exponential increase in the users' demands, and also to offer new features with the goal of stimulating the market, the mobile operators were forced to develop new techniques and technologies.

2.1 MIMO technology

As the world watches the mobile communications evolution, there is the necessity to develop technologies that can support it. This development is not only directed to the network itself, it also includes the development of the terminal devices. In this particular development, one fundamental component is the antenna.

The traditional wireless communication systems are based on the use of two antennas, one in the transmitter and another one in the receiver. This system is designated as Single-Input Single-Output (SISO). A SISO system doesn't require any complex processing, nevertheless this reflects on its limited ability to deal with fading when compared to other systems.

The Single-Input Multiple-Output (SIMO) is a system where the transmitter has a single antenna and the receiver has multiple antennas. It is often used to enable the receiver to capture signals with different delays to oppose the effects of fading, taking advantage of the receive diversity [2].

Multiple-Input Single-Output (MISO) is the opposite of SIMO. In this case a MISO system provides multiple transmit antennas to enable transmit diversity, which makes it possible for the receiver to optimize the acquired signal, to receive the required data. The use of MISO has the benefit of moving the processing from the receiver to transmitter. For example, in cellphone cases, its size, cost and battery life are reduced since that the use of a single antenna is compensated by the base station antennas.

MIMO is an efficient transmission technology used in modern wireless communication. As the name implies, MIMO uses multiple antennas for transmission and reception of a signal. The combination of multiple transmission sources provide improvements in both channel robustness, as well as channel throughput. Full MIMO systems are able to improve significantly the performance. However this comes with the cost of additional processing and the increase in the number of antennas [3].

Wireless technologies are using MIMO to provide spectral efficiency and increase the capacity and reliability. Examples of these technologies are the Wireless Fidelity (Wi-Fi), Long Term Evolution (LTE), or the more recent 5G and Internet of Things (IoT) [4]. Figure 2.1 shows the different technologies formats that were explained.

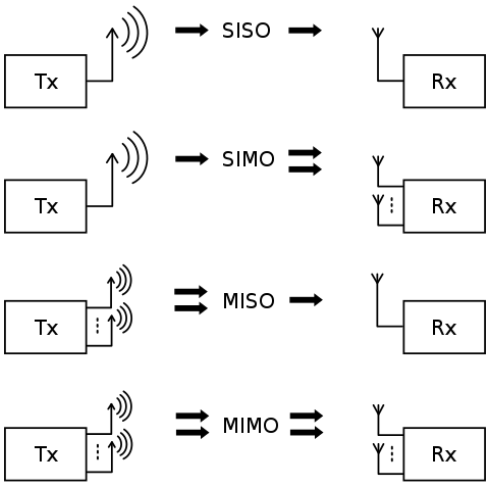

Figure 2.1: MIMO formats (adapted from [5])

Capacity wise, for a Additive White Gaussian Noise (AWGN) channel, the maximum capacity is given by equation 2.1 [6]:

$$C = log_2 (1 + SNR) \tag{2.1}$$

where SNR is the signal to noise ratio.

However using a MIMO system with multiple antennas is possible to increase the channel capacity to transmit data without overstepping Shannon's theorem [7]. In [8] is simulated the capacity of a MIMO system over Rayleigh fading channel with different number of transmit and receiver antennas. The plot of the channel capacity per SNR for different numbers of antennas is on figure 2.2.

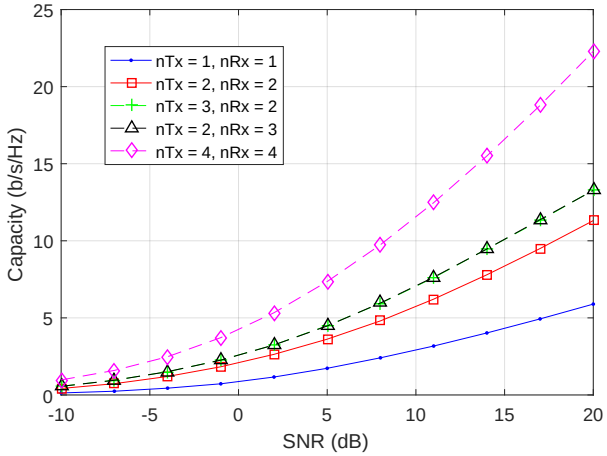

Figure 2.2: Average capacity of a MIMO system for different number of TX-RX antennas

The results on figure 2.2 demonstrate that for a higher number of antennas on the MIMO system, the higher the system capacity.

2.1.1 Antenna diversity

The employ of a MIMO system makes it possible to transmit and receive multiple data streams simultaneously, improving the throughput and consequently the Signal to Noise Ratio (SNR). However a channel affected by fading will have an impact on the SNR. As digital data is transmitted, the downfall of it means that the error rate will grow. The diversity's principle is to improve the quality and reliability of a wireless link, providing the receiver with multiple versions of the same signal. If these different versions of the signal can be made to be affected in different ways by the signal path, the probability that the signals will all be affected at the same time is considerably reduced.

Antenna diversity is utilized to lower the multipath interference effects, leading to a wireless connection enhancement. The classical techniques are the result of different diversity components combined: spatial diversity, frequency diversity, time diversity (multipath diversity), polarization diversity and pattern diversity.

Spatial diversity (figure 2.3) uses multiple antennas in different space positions to receive the same signal, originating from different connection paths. After the signals are received from the multiple antennas, they are combined to reduce the fading effect, taking advantage of different multipath fading in all channels.

Frequency diversity (figure 2.4) uses different carriers to transmit the same signal. Although it can be used to reduce the fading effect, this technique requires a larger bandwidth.

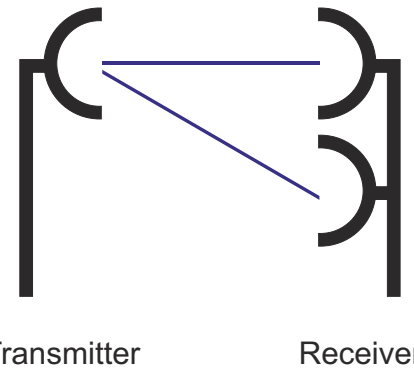

Figure 2.3: Spatial diversity scheme

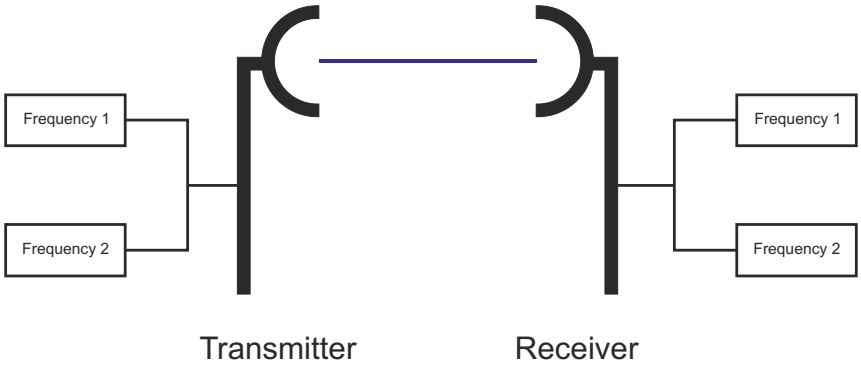

Figure 2.4: Frequency diversity scheme

Polarization diversity (figure 2.5) can be achieved by having two orthogonal polarizations (for example horizontal/vertical or +/-45°), providing almost uncorrelated signals in a scattering environment.

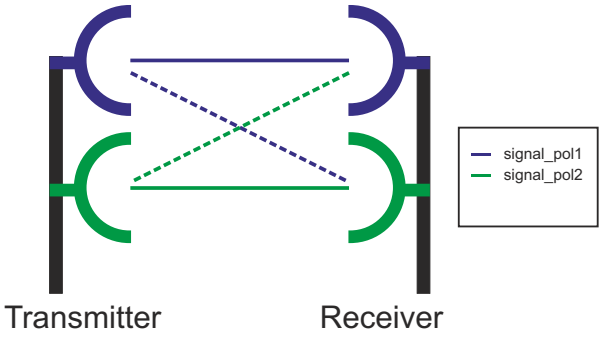

Figure 2.5: Polarization diversity scheme

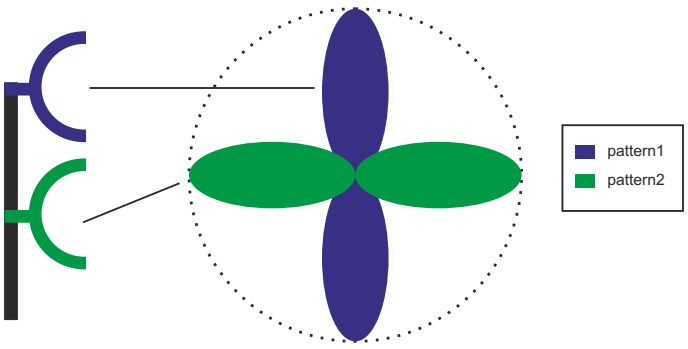

Figure 2.6: Pattern diversity scheme

Pattern diversity (figure 2.6) if two or more antennas with different radiation patterns are used.

2.1.2 MIMO parameters

When analysing a MIMO antenna system design there are some parameters that need to be evaluated, namely the Envelope Correlation Coefficient (ECC), the Diversity Gain (DG), Mean Effective Gain (MEG) and Multiplexing Efficiency (ME).

Envelope Correlation Coefficient

The ECC is the representation of how independent two antennas' radiation patterns are [9]. The correlation value would be 1.0 if they are the exact same; if they are completely independent, the correlation would be 0. As such, for MIMO applications the closer to 0 the better ECC. ECC is given by equation 2.2 [9]:

$$ECC = \frac{A_1}{A_2 \times A_3} \tag{2.2}$$

where A_1, A_2 and A_3 are given by equation 2.3, 2.4 and 2.5 respectively.

$$A_1 = \left| \oint \left[XPR \cdot E_{\theta 1}(\Omega) E^*_{\theta 2}(\Omega) P_\theta(\Omega) + E_{\phi 1}(\Omega) E^*_{\phi 2}(\Omega) P_\phi(\Omega) \right] d\Omega \right|^2 \tag{2.3}$$

$$A_2 = \oint \left[XPR \cdot E_{\theta 1}(\Omega) E^*_{\theta 1}(\Omega) P_\theta(\Omega) + E_{\phi 1}(\Omega) E^*_{\phi 1}(\Omega) P_\phi(\Omega) \right] d\Omega \tag{2.4}$$

$$A_3 = \oint \left[XPR \cdot E_{\theta 2}(\Omega) E^*_{\theta 2}(\Omega) P_\theta(\Omega) + E_{\phi 2}(\Omega) E^*_{\phi 2}(\Omega) P_\phi(\Omega) \right] d\Omega \tag{2.5}$$

where Ω=(θ,ϕ) and

$$XPR = \frac{P_V}{P_H} \tag{2.6}$$

is the Cross Polarization Ratio (XPR), the ratio between mean incident powers of the vertical and horizontal polarized incident radio waves received, the $P_\theta(\Omega)$ and $P_\phi(\Omega)$ describe the angular density of the incident power.

Since an isotropic power distribution over all angles is an unlikely model for ground based mobile communication, it is assumed a Gaussian distribution over the elevation

angle and uniform on azimuth. The Gaussian distribution can be described independently for the vertical and the horizontal components; In figure 2.7 the two distributions, for vertical polarization waves and horizontal polarization waves are illustrated.

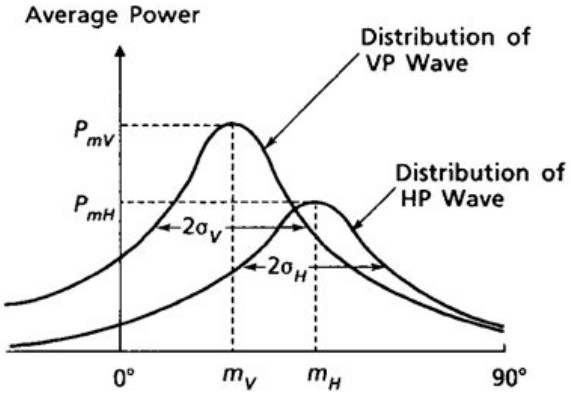

Figure 2.7: Gaussian distribution for vertical and horizontal polarizations waves

The m_V and m_H are, respectively, the mean elevation angle of each vertical polarization and horizontal polarization wave distribution observed from the horizontal direction. σ_V and σ_H are, respectively, the standard deviation of each vertical polarization and horizontal polarization wave distribution.

It should be noted that the elevation can take on negative values since mobile antennas usually operate at a certain position above the ground, that being the reason why the distribution functions have negative angles in figure 2.7.

Assuming high efficiency antennas and uniformly distributed incoming waves ($P_\theta(\Omega)$= $P_\phi(\Omega)$=1), and cross polarization ratio equal to 1 (XPR = 0 dB), the method for calculating the ECC is reduced to equation 2.7:

$$ECC = \frac{\left|\iint_{4\pi}\left[\vec{F}_1(\theta,\phi) \bullet \vec{F}_2(\theta,\phi)\right] d\Omega\right|^2}{\iint_{4\pi}\left|\vec{F}_1(\theta,\phi)\right|^2 d\Omega \iint_{4\pi}\left|\vec{F}_2(\theta,\phi)\right|^2 d\Omega} \tag{2.7}$$

where $\vec{F}_i(\theta,\phi)$ is the radiation pattern of the antenna and $\bullet$ represents the Hermitian product. For the same conditions ECC can also be obtained from the S-parameter with the same conditions using 2.8 [10]:

$$ECC = \frac{|S_{11}^* S_{12} + S_{21}^* S_{22}|^2}{(1-(|S_{11}|^2+|S_{21}|^2))(1-(|S_{22}|^2+|S_{12}|^2))} \tag{2.8}$$

where S_{11} and S_{22} are the input match values for port one and port two respectively, while S_{21} and S_{12} denote the inter port coupling. The lower the ECC value, the higher

the diversity gain achieved. If the MIMO system is composed by more than two antennas, ECC must be computed for each 2 antenna pair.

Diversity Gain

Diversity Gain (DG) represents the improvement of the signal to noise ratio of the diversity antenna system, when compared to the SNR from one single antenna system [11].

In order to optimize the SNR in a diversity scheme, the output signals can be combined in several ways such as Maximal Ratio Combining (MRC) Equal Gain Combining (EGC), or Selection Combining (SC). These techniques are shown on figure 2.8.

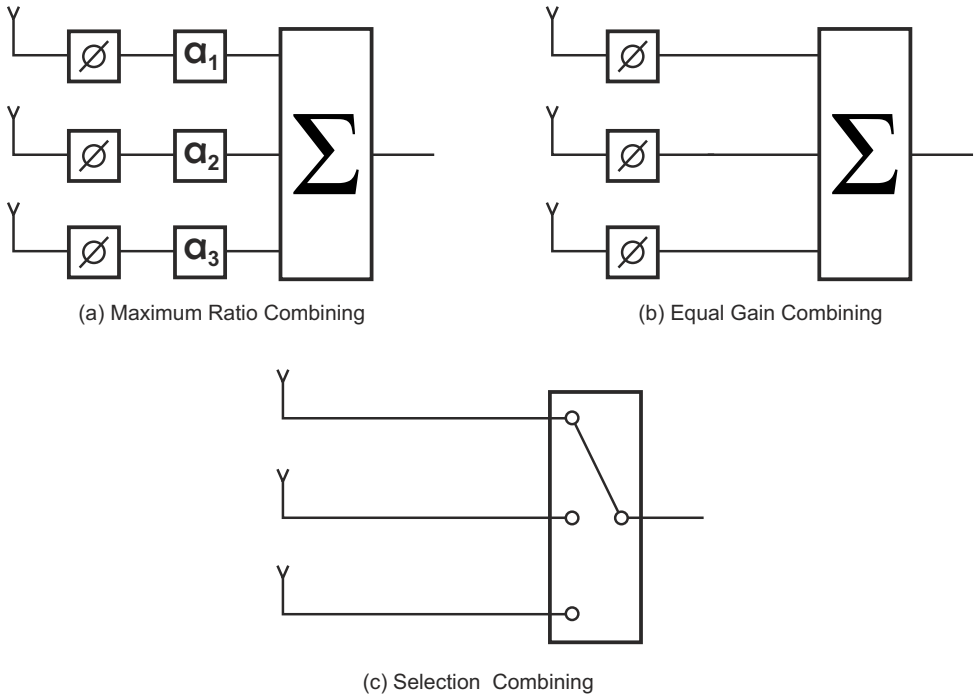

Figure 2.8: Methods of combining signals for diversity gain

In Maximum Ratio combining each signal branch is multiplied by a weight factor that is proportional to the signal amplitude. This means that the weak signals are attenuated and the strong ones are amplified. All the signals must be co-phased before being summed.

In Equal Gain Combining, each signal branch weighted with the same factor. All signals are co-phased to provide equal gain combining.

The selection combining selects the strongest received signal in branches. The principle is that,at any given moment of time, it picks up the branch with the highest SNR.

The diversity gain can also be obtained from the ECC parameter (equation 2.9:

$$DG = 10\sqrt{1 - ECC} \tag{2.9}$$

For two uncorrelated antennas and an accepted bit error rate of 1%, the maximum theoretical diversity gain is 10 dB with the selection combining technique; the correlation between the two antennas is the gain reduction factor.

Multiplexing Efficiency

Multiplexing Efficiency characterizes the efficiency between two antennas of the MIMO system. The multiplexing efficiency defines the loss of power efficiency when using a MIMO antenna to achieve the same channel capacity as that of an ideal array in the same propagation channel [12]. This parameter can also be obtained from the ECC and the total efficiencies of the two antennas (η_1) and (η_2) according to the equation 2.10 [13]:

$$ME = \sqrt{\eta_1\eta_2(1 - ECC)} \tag{2.10}$$

Mean Effective Gain

The Mean Effective Gain (MEG) is the ratio of the average power received by the antenna in a mobile propagation channel to the sum of the average powers that would be received in that same environment by two isotropic antennas, vertically and horizontally polarized, respectively [14]. It is expressed as shown in equation 2.11.

$$MEG = \frac{P_{rec}}{P_V + P_H} \tag{2.11}$$

MEG is a statistical measure of antenna gain that takes into account the effects of the radiation power pattern, the antenna total efficiency and the propagation effects and is given by [15] :

$$MEG = \int_0^{2\pi}\int_0^{\pi}\left(\frac{XPR}{1+XPR}.G_\theta(\theta,\phi).P_\theta(\theta,\phi) + \frac{1}{1+XPR}G_\phi(\theta,\phi).P_\phi(\theta,\phi)\right).sin\theta.d\theta.d\phi \tag{2.12}$$

where $G(\theta)$, $G(\phi)$, $P(\theta,\phi)$ and $P(\theta,\phi)$ are the elevation and azimuth components of antenna power gain patterns, and angular density of the incident power respectively.

For an urban environment the distribution parameters are [14]: m_V=20^o, σ_V=42^o, m_H=50^o, σ_H=90^o.

2.2 Mobile system antennas: state of the art review

In this section it will be presented some papers that include antenna designs from simple monopoles to MIMO antenna systems. It will reflect some of the work that was done in the mobile antenna's field in the last years.

2.2.1 Single band antennas

In [16] it was proposed a miniaturized Planar Inverted F-shaped Antenna (PIFA) antenna, for the 2.4 GHz Wireless Local Area Network (WLAN) band. The antenna geometry was developed based on the planar inverted-F antenna configuration. Although measurement results show the bandwidth, gain, and radiation efficiency characteristics meet WLAN specifications, the fact that makes use of such depth is not really viable to a MIMO system to a mobile phone. Being designed for the Industrial, Scientific and Medical (ISM) band, it only uses a single band, being not viable to this MSc.

In [17], a single band slotted microstrip patch antenna is presented. The proposed antenna is a simple structure, low cost and small size. The small size of antenna operates the single band frequency. Due to the design consists in cutting the H and E slots, the center frequency is at 59.93 GHz with bandwidth of 4.028 GHz. This antenna have a gain of 5.42 dB for the millimeter wave wireless application.

A PIFA design for LTE is presented on [18]. This design has a separate air gap, with a strip connecting the ground to the planar element. The antenna is optimized to cover the bandwidth centred at 2.6 GHz. This antenna has a small size, and has some parameters that allow to configure its frequency, with an antenna's gain of 4.9 dB. The drawback of using a PIFA antenna is that it has a narrow bandwidth.

The design method using shared dipole to design a wide band and high isolated dual-polarized antenna is presented in [19]. When compared with the traditional crossed dipole antennas, it has a similar high isolation within a more compact size.

2.2.2 Dual band antennas

[20] introduces a multi-band antenna that operates on 2.4 GHz and 5.8 GHz. The antenna has a T-shape, where the length of each arm allows to tune the work frequency.

The shorter arm is responsible for the higher frequency (5.8 GHz) and the larger one for the lower frequency (2.4 GHz). This type of design makes it difficult to be adjusted, considering that resizing any arm's length alters the resonant frequency of the other arm.

[21] proposes a F-shaped monopole antenna that has a simple geometry where there are two resonant paths: the shorter path (feed point - lower arm) generates the higher operating band; the longer path (feed point - higher arm) generates the lower operating band. The simulated and measured results include the input match and the radiation patterns. Similar to the T-shape antenna [20], resizing it is not trivial.

[22] presents the design of a single feed multiband printed monopole antenna array using fractal geometry. The multiband operation is achieved by a suitable chosen of the size and iteration of the fractal geometry. During this work, it is found that adding a rectangular stub on the ground plane, the impedance match of the antenna can be improved with little influence on the original resonant frequencies.The experimental results show that it can operate from 2.32 to 2.49 and from 5.1 to 5.88 GHz, which covers the required bands for IEEE 802.11a/b/g (2.41-2.48 GHz, 5.15-5.35 GHz and 5.725-5.875 GHz) applications.

A dual-band Inverted F-shaped Antenna (IFA) with Tunable Inductor and Capacitor (TIC) for 5G is proposed on [23]. The results show two frequency ranges where the input match is better than -15 dB, 2.74-3.74 GHz and 4.44-5.0 GHz, covering the 5G spectrum in China. This paper gives special attention to the input match values and the frequency range that it covers, not mentioning other important parameters, like the antenna's resulting gain.

2.2.3 Single band MIMO antennas

A three element single band PIFA system in the 28 GHz is presented on [24]. Results show that the proposed antenna has a bandwidth from 27.73 GHz to 28.54 GHz. Other important parameters in any wireless communication system such as ECC, DG, MEG, and Multiplexing Efficiency (ME), have been calculated, revealing that the prototype is a viable option.

A compact monopole slot MIMO antenna integrated on a 2.4 GHz WLAN module for Universal Serial Bus (USB) dongle applications is presented on [25]. This study focus on the design and implementation of the MIMO antenna in a multi-layered Printed Circuit Board (PCB). To ensure a high isolation between the two closely spaced MIMO antennas on a restricted antenna area it was introduced a T-shaped dent from the top

edge of the antenna area. The suppression of the coupling between the MIMO antennas has led to a better throughput results.

It has been designed a compact Inverted-L antennas array for WLAN 5.8 GHz applications in [26]. Using the neutralization technique it was possible to have high isolation between the two antenna elements and to provide impedance matching as well.

In [27] is presented a fractal compact MIMO antenna, fed by a microstrip line, provide polarization diversity. The realized diversity performance and isolation demonstrates good agreement that the proposed antenna is suitable for implementation in MIMO application.

2.2.4 Multi band MIMO antennas

In [28] it is used two C-shaped monopoles for WLAN applications. Resorting to neutralizing techniques is possible to achieve a high isolation between the two radiators. With a good isolation level (-12dB) it is also possible to operate on dual-band of the Wi-Fi bands (2.4 GHz and 5.2 GHz), making use of Radio Frequency (RF) switchers as neutralizing technique to provide the isolation.

[29] introduces a quad band planar microstrip-line fed antenna. The prototype consists of 3 different monopole antennas. The first antenna is a monopole with an inverted U shape that works at the 800 MHZ and 1.8 GHz. The second one has L-shape and according to its length works at 2.4 GHz. The third monopole works at 3.5 GHz, being the shortest one. This prototype is a reconfigurable PIFA antenna, where PIN switches were placed on each arm that works at different band. Re-configurable antennas are a solution for the required functionalities within a very limited space, in cases such as the mobile devices. In this paper is also presented a two-element antenna system for MIMO applications, where is measured the S-parameters.

In [30] it was designed a low profile dual-band MIMO antenna. This design focus on having an isolation between the antennas is over 10 dB and a low ECC, providing the antenna system a high efficiency and a good MIMO performance. The chosen frequencies were 900 MHz and 1800 MHz, each with a bandwidth of 100 MHz.

A MIMO antenna system composed by 2-element fractal shaped monopole antennas is introduced in [31]. To improve the matching and isolation between the antenna elements a T-shaped stub was used. The proposed antenna configuration also provides beam tilting over the operating frequency due to the presence of the T- shaped stub, thus creating pattern diversity. The results shows that the proposed antenna operates in the frequency range of 3.1 - 7.5 GHz.

The paper [32] shows a study of multi-slot decoupling techniques that can improve the performance of dual-band MIMO array system for 5G terminals applications. It was establish the comparison between designs with different approaches, including Single-band Neutralization line or Dual-band Multiple slots as decoupling techniques. The Dual-band Multiple slots prototype was created and measured, where the results confirm the values obtained on the simulation. This work regards the input match limit as -6dB, not meeting this project's standards.

In [33] proposed MIMO antenna system consists of two meander line monopole, designed to be bent opposite to one another to reduce the mutual coupling, and covers the Time Division - Long Term Evolution (TD-LTE) 2.57-2.62 GHz frequency band; and the other Time Division - Synchronous Code Division Multiple Access (TD-SCDMA) (1.8-2.4 GHz) antenna system is based on the PIFA antenna structure with a small radiation sheet metal. On the basis of the simulated results, the proposed system has a high isolation (26.7 dB) at the central frequency of 2.6 GHz. The proposed antenna system can be used for TD-LTE dual-mode mobile terminal combined with MIMO technology. The chosen bandwidth is not compatible with our goal, but the results show that the antenna radiation efficiency can reach to 98.12%.

Antennas of two fractal elements were designed and fabricated in [34]. Although the size of the designed antenna prototypes is small and the elements are positioned too close to each other, correlation coefficients lower than 0.1 and satisfactory levels of Mean Effective Gain have been obtained. These makes the system suitable for portable devices used for local communication networks.

A MIMO antenna with improved isolation using a decoupling network for LTE mobile application is proposed [35]. The proposed MIMO antenna has a 6 dB input match bandwidth and the isolation characteristic is higher than 11 dB over the whole LTE band. The ECC was less than 0.4, meaning that the proposed decoupling network can be a good candidate for a MIMO antenna system requiring high isolation characteristic. Despite being a small scale design as requested, the project is expected to have a input match of 10 dB or higher, where this design doesn't meet the requirements.

In [36], a Half Shaped Cubical Parasitic Antenna design is proposed for MIMO mobile terminal application. This design covers high frequency bands that have been planed for 5G communication system, using 3 PIFA elements at single port to resonate at multiple higher frequency bands with different radiation patterns. Multiple resonance frequencies in the 4 GHz to 14 GHz range have been achieved with an acceptable reflection coefficient. Stable pattern reconfiguration and low ECCs at specified frequency bands indicate that this antenna performs well and is suited for MIMO mobile terminals. This design was not fabricated and measured, which means that the prototype's

results haven't been proven to match the theoretical ones.

In [37], an eight-port hybrid 5G/WLAN MIMO antenna array with hexa-band operation for mobile handsets has been investigated. The proposed design is a low profile and compact for multi-band and multi-mode operations. It can cover LTE bands 4.2/4.3/4.9 GHz band and the entire WLAN 2.4/5.2/5.8 GHz bands. Besides, ECC values of the proposed MIMO antenna array are less than 0.12 over the desired bands. However, the threshold defined for the input match is 6 dB and like other previous designs, it doesn't meet the standards for this project.

A small, tunable antenna system for MIMO operations in the 1800 MHz/1900 MHz UMTS bands has been proposed on [38]. A ground plane and strip arrangement was used to decrease the mutual coupling between the antenna elements. The predicted antenna performances with and without the decoupling mechanism have been presented. This design excels for its simplicity, but has a very narrow bandwidth for a single frequency. This design wasn't manufactured, meaning that there real environmental tests haven't been performed.

In [39] it's described the design considerations from a Wi-Fi system perspective, including from the mobile devices' view. As already mentioned, one of the biggest constraints is the limited space on the terminal and considering the space shared with other elements that are conductive and lossy, this reduces the antenna's efficiency. On this paper it is also showed two antenna configurations for mobile devices, where antenna diversity is applied. In both cases the inverted-F antenna design is used, however the placement of the second radiating element is differentiated. In the first case, the second antenna is positioned along the ground plane, achieving spatial and polarization diversity. For case two the antennas are placed back to back, meaning that the distance between them is closer than on the first case, which will limit the spatial diversity. The antennas are also placed with the same orientation, so there is no polarization diversity. The results obtained show that the system using the spatial and polarization diversity is better, which complies to the WLAN frequency specifications as shown on the S-Parameters, and a better diversity performance when analysing the ECC of the antenna systems.

A compact four port reconfigurable MIMO antenna design for IEEE 802.11 applications is proposed in [40]. In one configuration the antenna provides 4-ports operating from 4.9-5.725 GHz with isolation between antennas greater than 14 dB. In the second configuration it provides a 2-port antenna operating at 2.4-2.5 GHz together with another 2-port antenna operating at 4.9-5.725 GHz. The antenna is simulated and measured, including radiation patterns, S-parameters, and signal correlations and branch power ratio between ports. This design makes use single band antennas for the system.

In [41], a dual band 2 element MIMO antenna is presented, covering the 2.4 and 5 GHz bands with a high port-to-port isolation. This design is based on planar inverted-F antennas and simulates its MIMO performance. This letter antenna only uses two ports.

In [42] the antenna operates at 4.9-5.725GHz with 4-ports and at 2.4-2.5GHz with 2-ports and utilizes a dual-band dual-port MIMO antenna to cover the 2.4/5GHz bands alongside two single band antennas to cover the 5GHz band.This paper presents the simulation and measurement results.

The described articles introduce different antenna's designs and antenna systems, where the focal points also differ from each other; some concentrate on the input match parameter, others on increasing the bandwidth available or the antenna's gain. This review aims to summarize the current thinking in mobile antenna's design field, leading to new perspectives on this issue, and allowing to frame theoretically this thesis' project.

3

Single port antenna

This chapter describes the design of a single port, dual-band antenna that will be the basic element used in the MIMO antenna. The design starts with two separate planar IFA antennas, one for each band and follows with the integration of these antennas in a single design, first with two independent feeds and finally with a single feed.

3.1 Single band antenna

The first step is to design a planar IFA antenna using EM simulation (CST Studio Suite will be used). This design is chosen due to its simple geometry and based on the state of the art review.

An Inverted-F Antenna (IFA) consists of a thin arm or wire shorted at one of the ends to the ground plane (see figure 3.1). The input impedance depends on the space between the shorting pin and the feed position, decreasing as the feed gets closer to the shorting pin. The length of the arm should be nearly $\lambda/4$ [43].

The performance of the IFA is similar to that of the slot antenna [43]. The width W of the shorting pin is small compared to the wavelength of the dieletric, usually $0.05\lambda \leqslant W \leqslant 0.1\lambda$ [43].

3.1.1 Planar IFA

To design the antenna to cover the Wi-Fi bands, the initial values for the parameters of W and L of the designs are calculated on equations 3.1 to 3.4.

$$L_{2.4GHz} = \frac{\lambda}{4} = \frac{3 \times 10^8}{4\sqrt{4.3}(2.44 \times 10^9)} = 14.8mm \tag{3.1}$$

$$W_{2.4GHz} = \lambda \times 0.1 = 5.9mm \tag{3.2}$$

$$L_{5GHz} = \frac{\lambda}{4} = \frac{3 \times 10^8}{4\sqrt{4.3}(5.4 \times 10^9)} = 6.7mm \tag{3.3}$$

$$W_{5GHz} = \lambda \times 0.1 = 2.7mm \tag{3.4}$$

The design of the antenna is on figure 3.1. Table 3.1 shows the initial dimensions for the 2.4 GHz and 5 GHz planar IFA antennas. The width of the feed line was chosen so that a 50 Ohm characteristic impedance is obtained when printed on a FR4 substrate and the width of the antenna traces were made equal to this dimension.

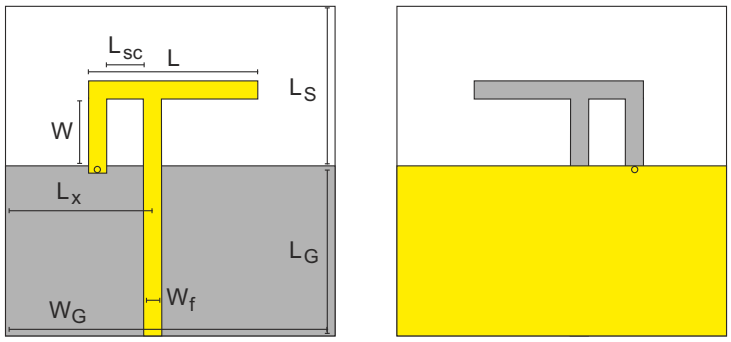

(a) front side (b) back side

Figure 3.1: Planar IFA antenna design geometry

Table 3.1: Planar IFA antenna initial dimensions for 2.4 GHz and 5 GHz band

	2.4 GHz	5 GHz
Parameter	Dimension [mm]	
L	14.8	6.7
W	5.9	2.7
L_{sc}	1	1
L_x	30	30
L_f	30	30
L_G	30	30
W_G	60	60
L_S	30	30

In figures 3.2 and 3.3 it is shown the input match at the 2.4 and 5 GHz bands, respectively. These results are achieved using the initial parameter dimensions on table 3.1, and it cannot meet the requirements. In order to cover the necessary frequency bands, the dimensions of the antenna are adjusted.

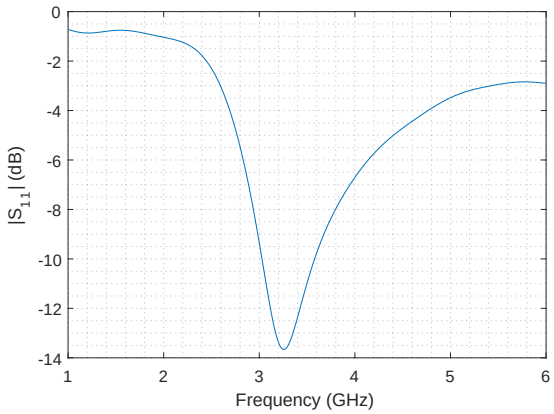

Figure 3.2: Planar IFA antenna S_{11} for 2.4 GHz band with initial dimensions

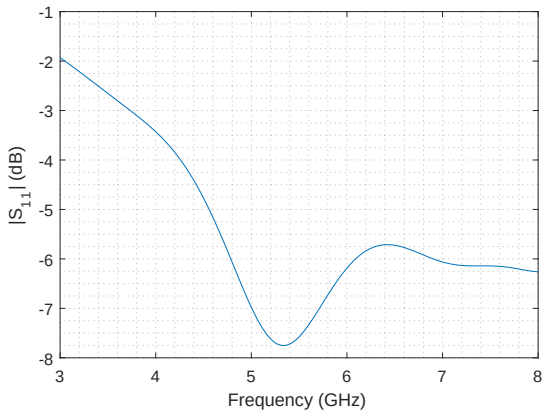

Figure 3.3: Planar IFA antenna S_{11} for 5 GHz band with initial dimensions

The S_{11} results for the 2.4 and 5 GHz bands after the dimensions adjustment are shown on figures 3.4 and 3.5 respectively. The Wi-Fi bandwidths are covered and have a good adaptation. The dimensions of the designs that obtain this results are indicated on the table 3.2. Table 3.3 summarises the frequency results for both antennas.

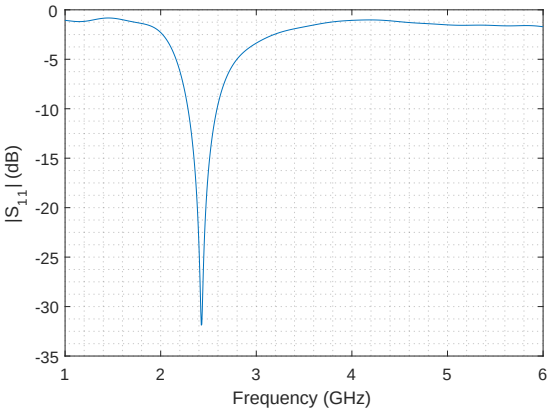

Figure 3.4: Planar IFA antenna S_{11} for 2.4 GHz band

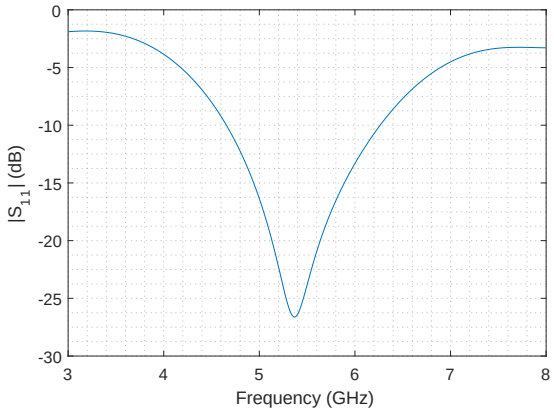

Figure 3.5: Planar IFA antenna S_{11} for 5 GHz band

Table 3.2: Planar IFA antenna initial dimensions for 2.4 GHz and 5 GHz band

	2.4 GHz	5 GHz
Parameter	Dimension [mm]	
L	27.5	15.3
W	11.2	2
L_{sc}	7	4
L_x	15.4	8.5
L_f	20	20
L_G	20	20
W_G	35	25
L_S	14.5	14.5

Table 3.3: Summary results of planar IFA antennas

	Bandwidth	fc [GHz]	S_{11}[dB]
2.4 GHz	300 MHz (12.32%)	2.44	-33.8
5 GHz	2060 MHz (38.36%)	5.4	-27.2

3.1.2 Planar IFA parametric study

To improve the design, the dimension parameters dependence is analysed. The input matching dependency on the several antenna parameters is shown from figure 3.6 to figure 3.12.

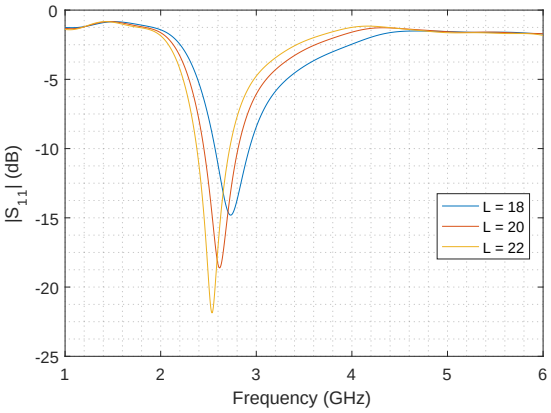

Figure 3.6: Planar IFA antenna S_{11} results for different L values

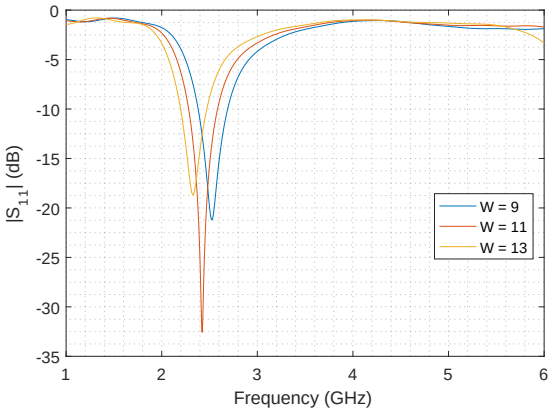

Figure 3.7: Planar IFA antenna S_{11} results for different W values

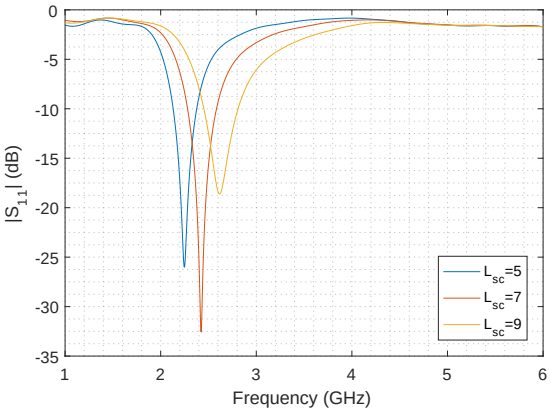

Figure 3.8: Planar IFA antenna S_{11} results for different L_{sc} values

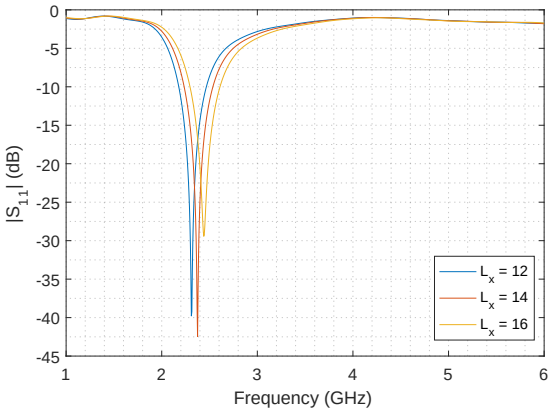

Figure 3.9: Planar IFA antenna S_{11} results for different L_x values

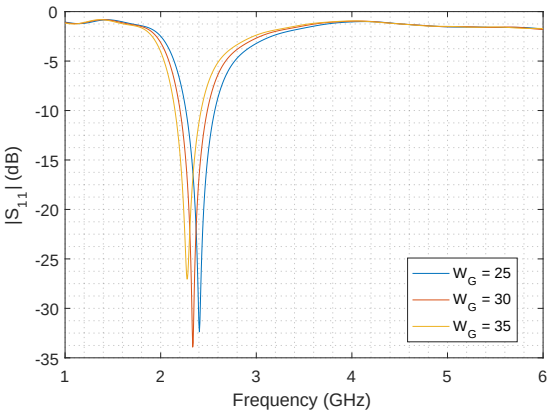

Figure 3.10: Planar IFA antenna S_{11} results for different W_G value

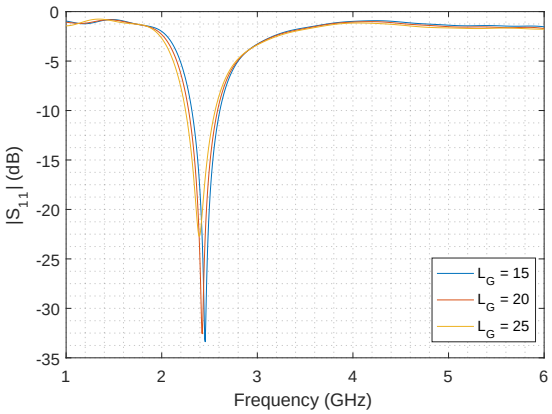

Figure 3.11: Planar IFA antenna S_{11} results for different L_G values

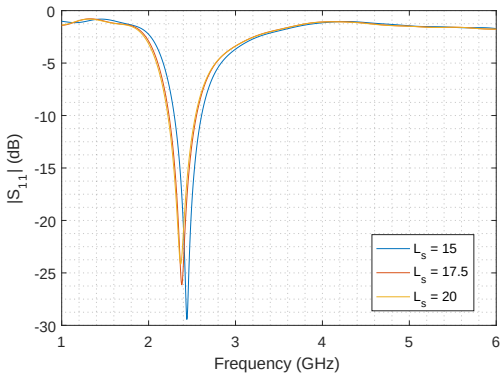

Figure 3.12: Planar IFA antenna S_{11} results for different L_s value

Analysing figures 3.6 and 3.7, increasing either dimension L or dimension W reduces the frequency of operation. The space between the arms results (figure 3.8) shows that increasing it makes the input match decrease and a shift for higher frequencies, however slightly increases the bandwidth. The other results show that the remaining parameters don't have a heavy influence on the input match.

3.2 Dual band IFA

The next step is to incorporate the two antennas (with the dimensions of table 3.2) on the same substrate. In the first stage, the two antennas are placed back to back with the same distance between them, fed independently by two ports. In the second stage, a unique port that feeds both elements is used. The third stage of the design combines the two elements with a shared short circuit arm. The final stage consists on having the two elements on the same direction, reducing the final dimensions of the IFA antenna design.

3.2.1 Dual port antenna

The first dual band design is shown on figure 3.13. Using the same dimensions as previously in the single band designs, the 5.4 GHz antenna is inverted to the left. The S_{11} and S_{22} results are presented on figure 3.14.

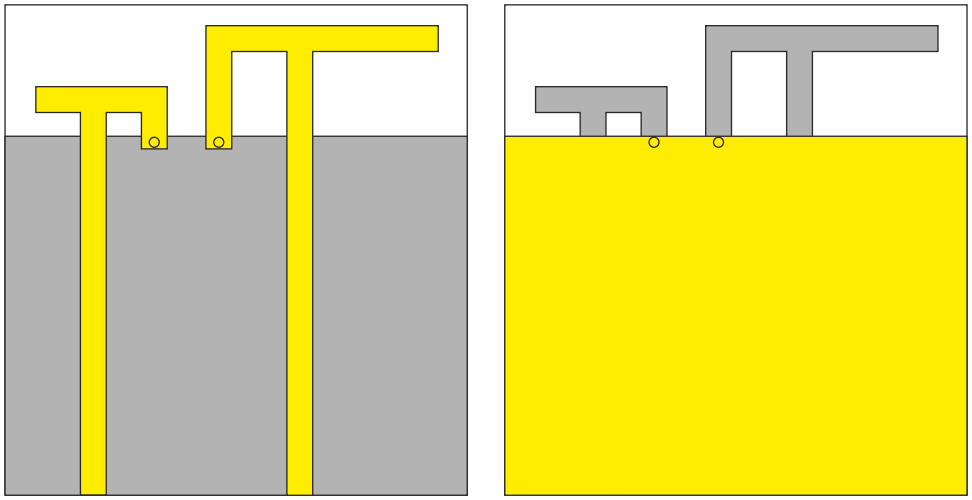

(a) front side (b) back side

Figure 3.13: Planar IFA dual band antenna - 2 ports design geometry

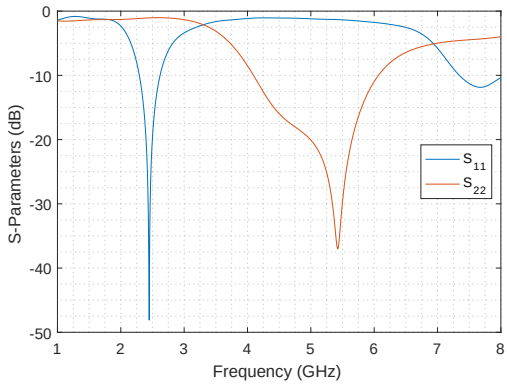

Figure 3.14: Planar IFA antenna dual band design - 2 ports S-parameters results

The results are as expected, following the outcome of the previous single band designs, covering the required bandwidths. As it embodies the two previous antenna designs, the dimensions increase to 6 x 5 cm. The next step is to link the two antennas' feed lines to the same port.

3.2.2 Single port antenna

The challenge of having only one port to feed the design is to have matching impedance (50 Ω) on the input of both antennas. It's necessary to achieve feed lines with a length that has a good matching level for both antennas and their respective frequencies. As the feed line divides into two, each line has to have a matching impedance for its own frequency and a mismatch for the other line frequency.

Table 3.4: Impedance values for different length feed lines

	Length	Z_{11}	Z_{22}
2.4 GHz	5	45.57+1.5i	398.01-388i
	10	50.41+1.7i	32.09-145.82i
	13	50.98+1.07i	15.57-96.42i
	15	51.15+0.65i	10.92-76.58i
	20	51.12-0.2i	5.82-45.68i
	25	50.71-0.77i	3.91-26.42i
	26	50.59-0.84i	3.68-23.23i
5 GHz	5	6.05-38.74i	50.96-1.37i
	10	3.8-4.87i	49.18-1.42i
	13	3.99+12.25i	48.48-0.61i
	15	4.73+25.09i	48.37+0.11i
	20	14.19+82.21i	49.37+1.52i
	25	578.05-220.59i	51.15+1.27i
	26	147.06-271.86i	51.41+0.95i

Looking at the table 3.4, it's possible to observe that a good length for the 5.4 GHz feed line is 5 mm; increasing it further makes the impedance values for this design not suitable. As for the 2.4 GHz antenna, the feed line's length can be adequate at 25 mm, giving it more dimension flexibility, when compared to the 5.4 GHz antenna's feed line length. The impedance at the lines intersection can be calculated using a parallel combination:

$$Z_{11}//Z_{22}(2.4GHz) = (50.71 - 0.77i)//(398 - 388i) = (43.71 - 12.08i)\Omega \tag{3.5}$$

$$Z_{11}//Z_{22}(5GHz) = (578.05 - 220.59i)//(50.96 - 1.37i) = (47.89 - 4.16i)\Omega \tag{3.6}$$

The design adjustments are showed on figure 3.15, where it's visible that there is only one feed line that supply the antenna. The size of the other dimensions of the design remain unchanged.

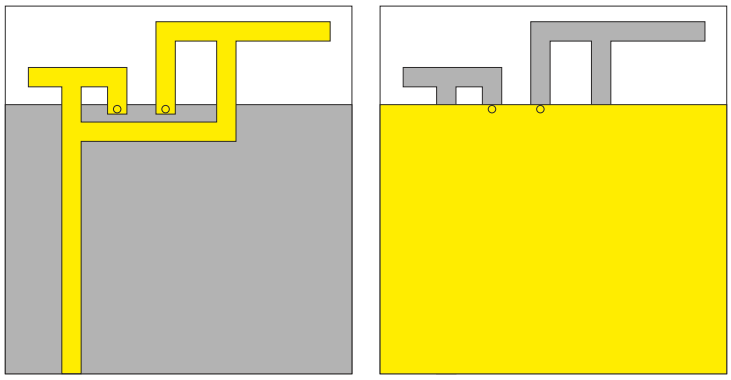

(a) front side (b) back side

Figure 3.15: Planar IFA dual band antenna - single port geometry

With this design, the result for S_{11} parameter is displayed on figure 3.16.

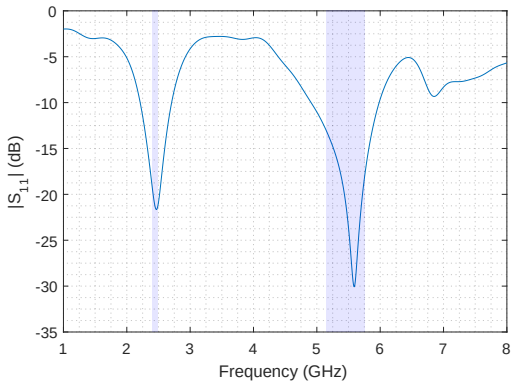

Figure 3.16: Planar IFA dual band antenna - single port S_{11} result

To start reducing the size of the antenna, the next step to take on the antenna design is to share the same short circuit arm, as shown in figure 3.17.

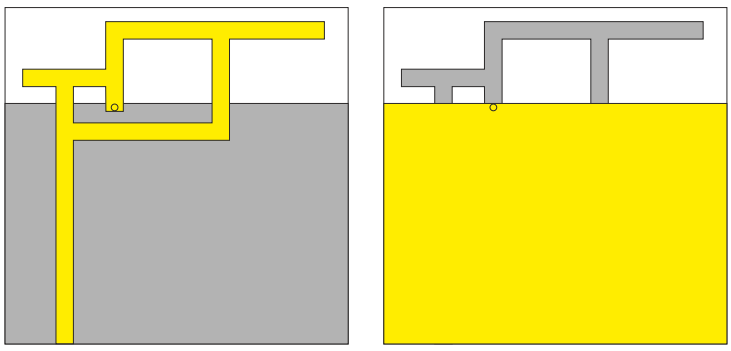

(a) front side (b) back side

Figure 3.17: IFA dual band - same short circuit arm geometry

Using the same parameter dimensions of the design of figure 3.17, the results on figure 3.18 are obtained and it is visible that the required bandwidths are covered.

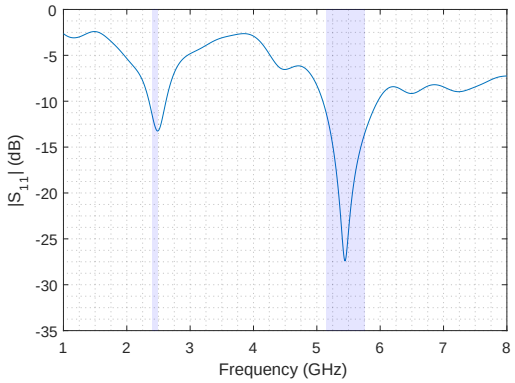

Figure 3.18: IFA dual band - same short circuit arm S_{11} result

3.2.3 Single port antenna compact design

The final step is to reduce the antenna's size even further by sharing the same feed arm and have the two arms facing the same side, as shown on figure 3.19. To reduce the antenna size, the longer arm (responsible for the frequency of 2.4 GHz) is bent. The antenna dimensions are those on table 3.5. After some tests, the S_{11} parameter on figure 3.20 is obtained, and the efficiency of it is on figure 3.21.

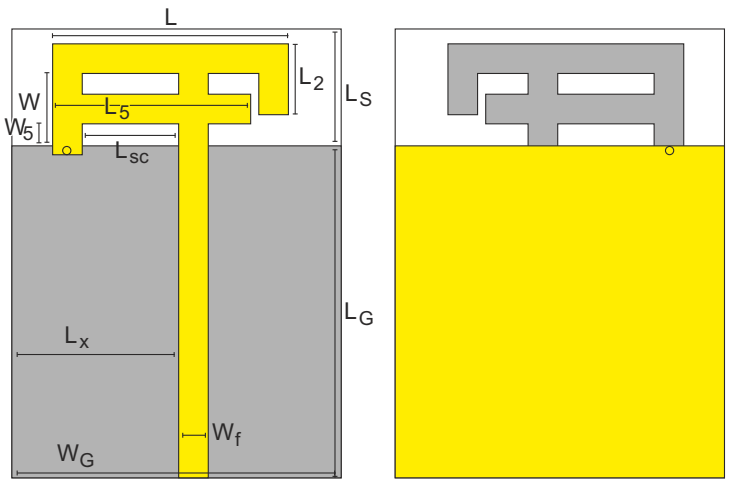

(a) front side (b) back side

Figure 3.19: IFA prototype design geometry

Table 3.5: IFA antenna dual band parameters

Parameter	Dimension [mm]
L	28.1
L_2	8.6
L_5	8.9
W	5.3
W_5	2
L_{sc}	4.75
L_x	20
L_f	25
L_G	25
W_G	40
L_S	12.3

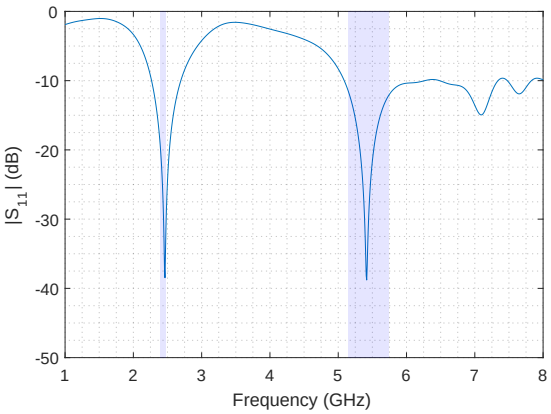

Figure 3.20: IFA prototype design S_{11} result

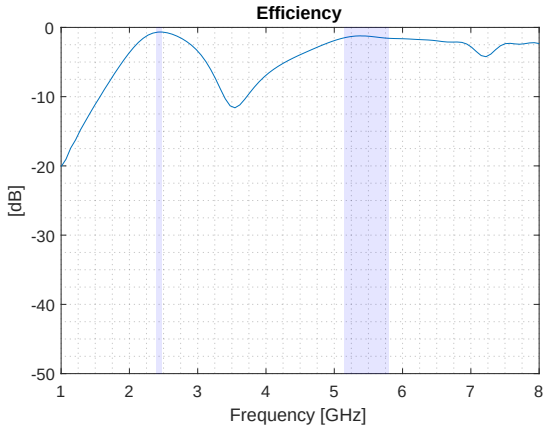

Figure 3.21: IFA prototype design efficiency results

Figure 3.22 shows the antenna positioning in the cartesian coordinate system. Figure 3.23 shows a 3D display of the radiation pattern at 2.4 GHz. Polar representation of the radiation pattern in principal planes are shown in 3.24 (plane XZ) and 3.25 (plane YZ).

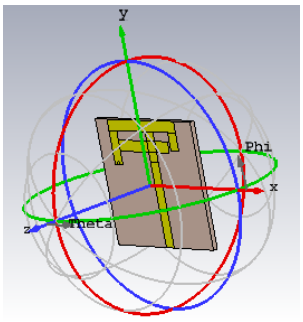

Figure 3.22: Spherical coordinate system - radiation pattern

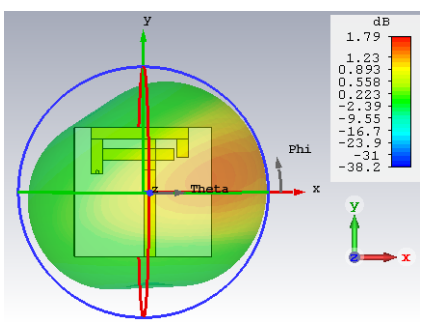

Figure 3.23: IFA Design 3D radiation pattern 2.4 GHz

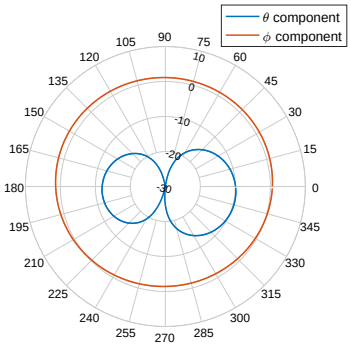

Figure 3.24: IFA design polar radiation pattern at plane XZ (2.4 GHz)

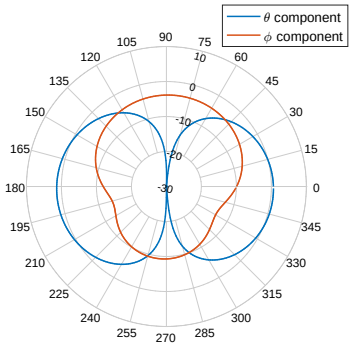

Figure 3.25: IFA design polar radiation pattern at plane YZ (2.4 GHz)

The 3D radiation pattern for 5.4 GHz is present on figure 3.26, with the polar representations of the radiation pattern on figures 3.27 and 3.28. The current density for both frequency bands is on figure 3.29

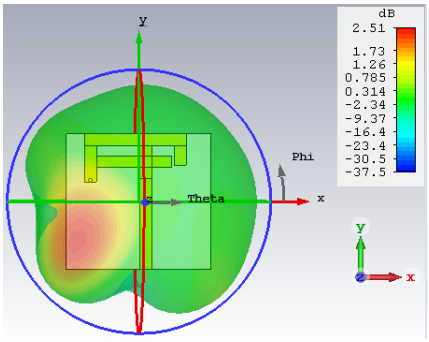

Figure 3.26: IFA design 3D radiation pattern (5.4 GHz)

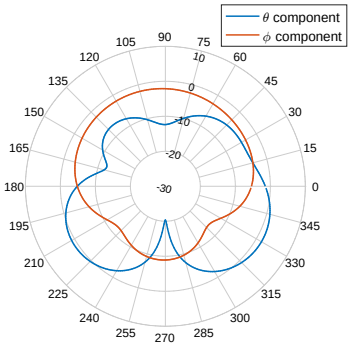

Figure 3.27: IFA design polar radiation pattern at plane XZ (5.4 GHz)

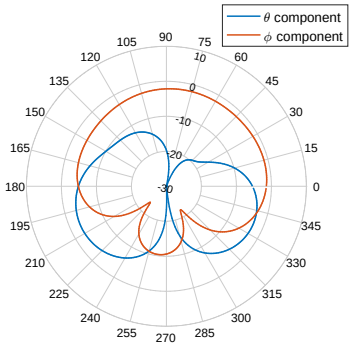

Figure 3.28: IFA Design Polar Radiation Pattern at plane YZ (5.4 GHz)

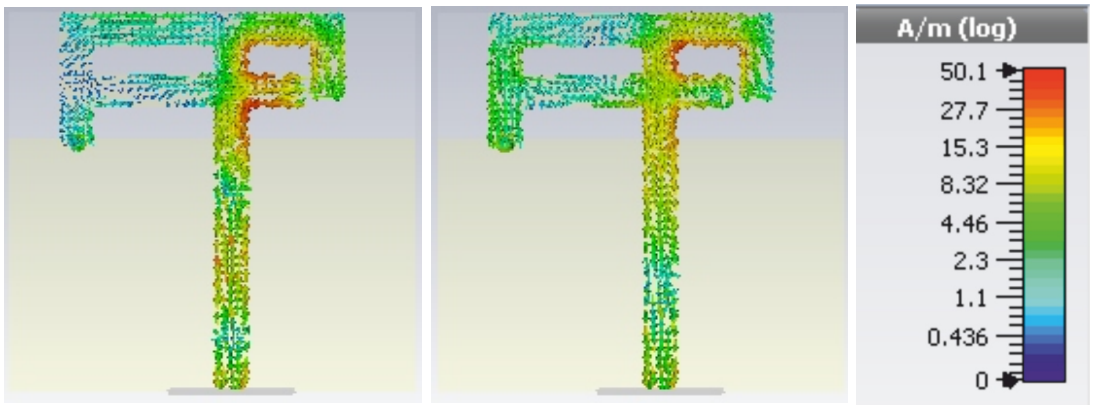

(a) 2.4 GHz band (b) 5 GHz band

Figure 3.29: Current density results for planar IFA

3.2.4 Manufactured Prototype

A prototype of this antenna was manufactured as shown on figures 3.30, and measured as shown 3.31.

(a) front side (b) back side

Figure 3.30: Planar IFA prototype

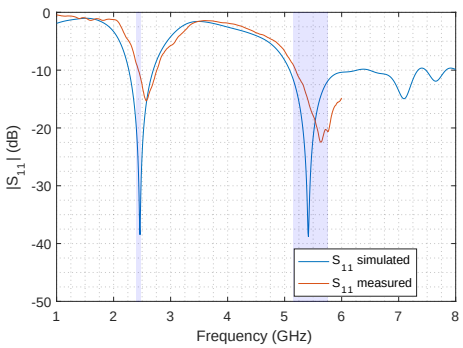

Figure 3.31: Planar IFA design S_{11} measured vs S_{11} simulated

Figure 3.31 shows a comparison between simulation and measured $|S_{11}|$. An offset is

visible when comparing the simulated and measured S_{11} results. A small summary of the main results are shown on tables 3.6 and 3.7. In the measured results, the 2.4 GHz bandwidth (2.43 GHz - 2.76 GHz) is slightly deviated from the simulation result. It can also be verified that the bandwidth is narrowed down (as can be seen on table 3.6). At the 5.4GHz band, the result is also deviated, where the measured bandwidth (5.18 - 6 GHz) is larger than the simulated results. The good agreement between simulation and measurement validated the proposed antenna.

Table 3.6: Summary results of the prototype antenna for 2.4 GHz

	Bandwidth (2.4GHz)	fc [GHz]	S_{11}[dB]
Simulated	430 MHz (17.73%)	2.42	-37.21
Measured	330 MHz (12.72%)	2.57	-15.32

Table 3.7: Summary results of the prototype antenna for 5.4 GHz

	Bandwidth (5.4GHz)	fc [GHz]	S_{11}[dB]
Simulated	1210 MHz (21.36%)	5.38	-45.8
Measured	>810 MHz (14.47%)	5.6	-22.3

4

Antenna design: MIMO system

In this chapter several MIMO antennas area presented with either 2 or 4 elements, using the antenna developed in chapter 3 as basic element. All the MIMO antennas share a common ground plane as the effect of different antenna element positioning will be evaluated through both input matching level and MIMO parameters.

4.1 Planar IFA with coaxial feed

Before moving to the MIMO designs, the planar IFA element is modified to include a coaxial port placed on the antenna's back like on the figure 4.1. A detailed view of the coaxial is shown in figure 4.2, with its dimensions and the dielectric ϵ_r on the table 4.1. The coaxial has an impedance of 50 Ω.

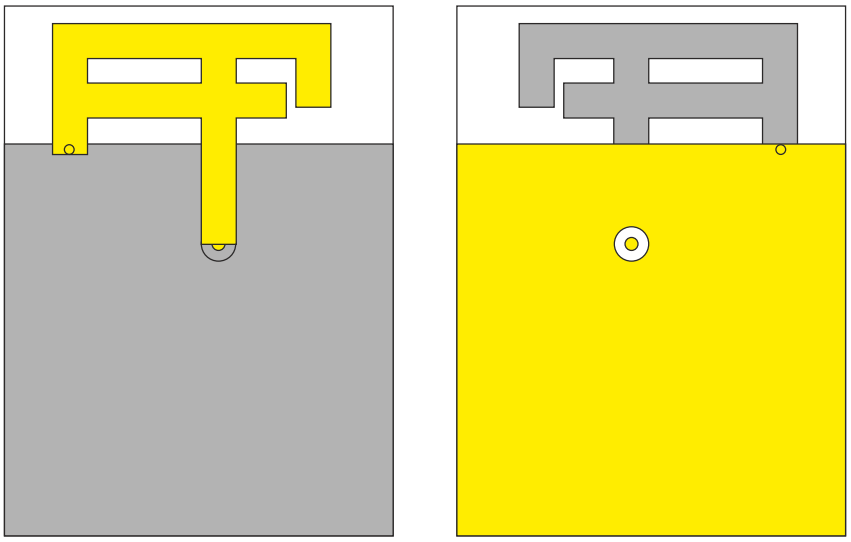

(a) front side (b) back side

Figure 4.1: IFA antenna dual band design geometry with coaxial feed

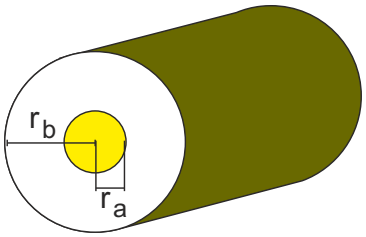

Figure 4.2: Detailed view of coaxial connector for feed antenna 4.1

Table 4.1: Planar IFA antenna coaxial characteristics

Characteristic	Value
r_a	0.65 mm
r_b	1.99 mm
ϵ_r	1.8

To make room to the several MIMO antenna elements, the ground plane has to be enlarged, and the input match results of this design are significantly affected by it. To

avoid a high dependence of the size of the ground, the design is altered like on figure 4.3. Figures 4.4 and 4.5 show how the input match changes when the ground plane dimension is increased. As it can be seen, although a larger ground allows for a small increase in the operating bandwidth at both 2.4 GHz and 5 GHz, the results are kept essentially the same.

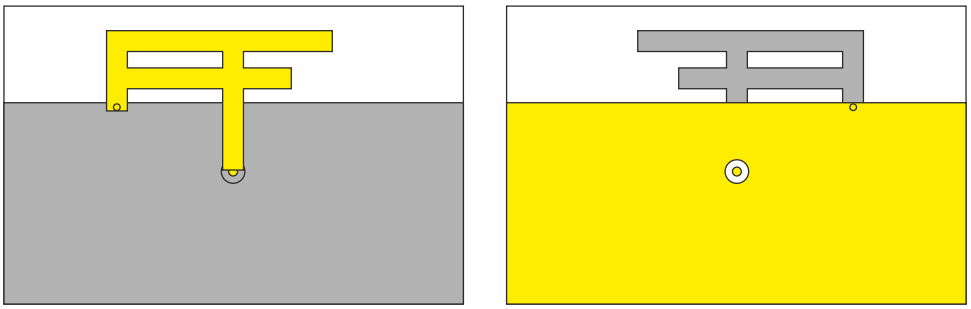

(a) front layer (b) back layer

Figure 4.3: Planar IFA antenna dual band final design geometry

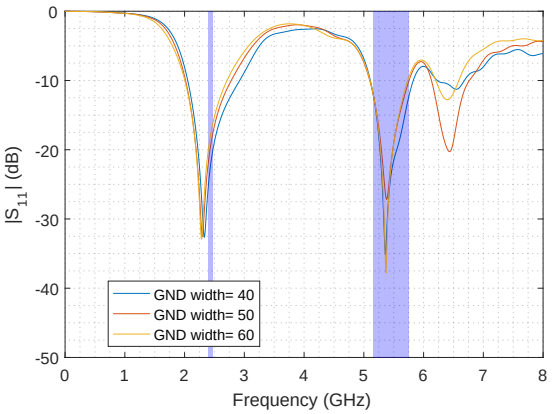

Figure 4.4: Planar IFA antenna dual band design S_{11} for different ground width values

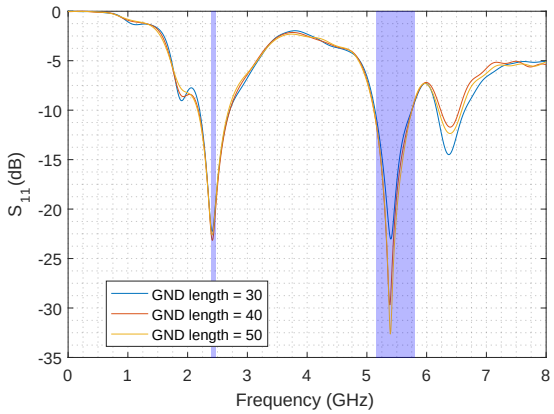

Figure 4.5: Planar IFA antenna dual band design S_{11} for different ground length values

4.2 Two element MIMO antennas

With the planar IFA antenna design concluded, the next step is to build a MIMO system with it. It is simulated different configurations of MIMO antennas of two elements, which are evaluated by their s-parameters and MIMO parameters.

4.2.1 Side by side configurations

These configurations have two antennas placed on the same ground plane, side by side.

Configuration 1

The first configuration is shown on figure 4.6, and its scattering parameters results are shown on figures 4.7 and 4.8.

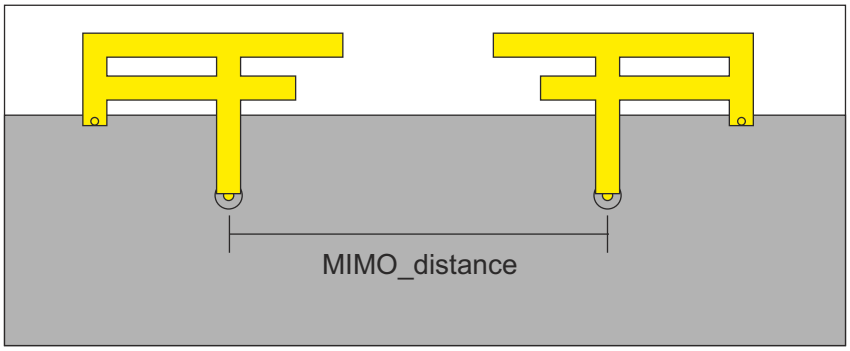

Figure 4.6: Side by side configuration 1

Due to the antenna symmetry, the input match results from port 1 and 2 are identical. The dependence of the antenna s-parameters on the distance between antennas is shown in figure 4.7 (S_{11}, S_{22}) and in figure 4.8 (S_{12}, S_{21}). The results show a slight improvement when the distance increases. The mutual coupling achieves a value of -14 dB, while the input match shows a result below the -10 dB for both bandwidths.

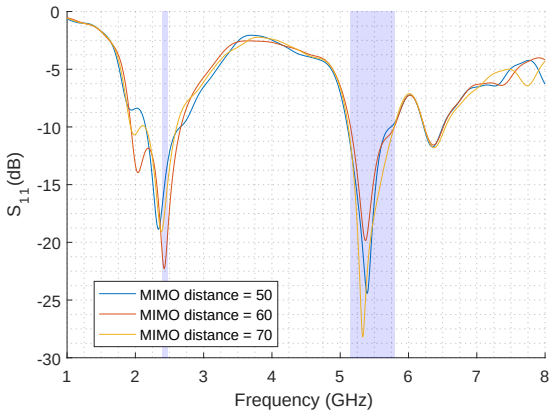

Figure 4.7: Configuration 1 distance variation S_{11} results

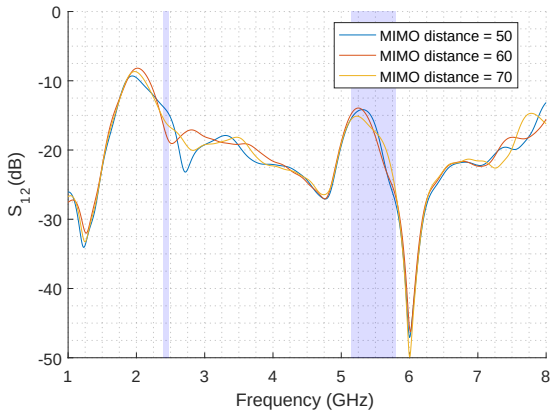

Figure 4.8: Configuration 1 distance variation S_{12} results

The theoretical MIMO parameters (ECC, DG, ME, MEG) are evaluated for the frequency bands of 2-3 GHz and 5-6 GHz. The results are shown, respectively, on figures

4.9, 4.10, 4.11 and 4.12.

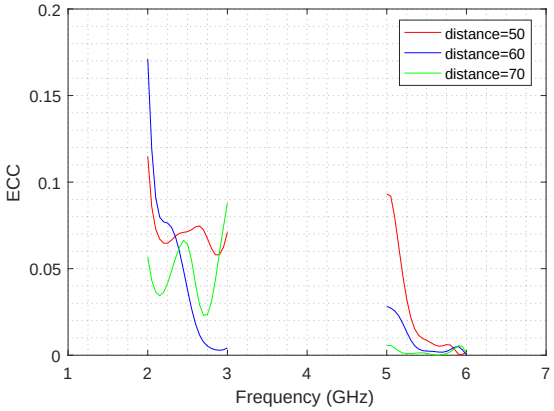

Figure 4.9: Configuration 1 ECC for different distances

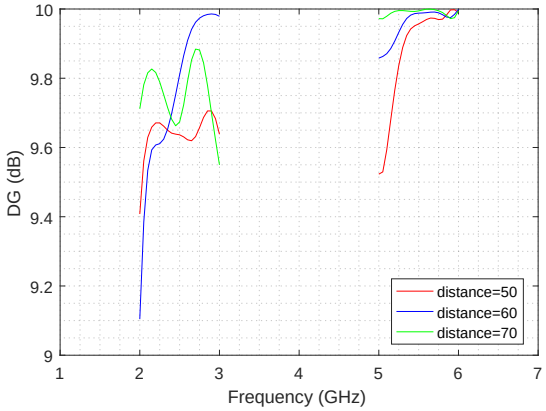

Figure 4.10: Configuration 1 DG for different distances

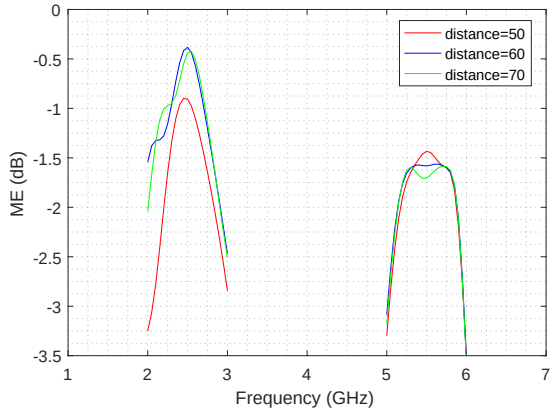

Figure 4.11: Configuration 1 ME for different distances

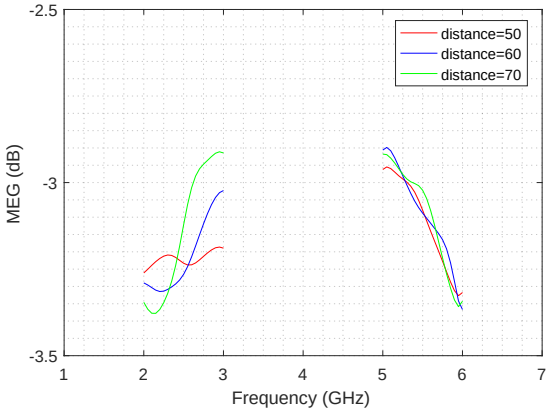

Figure 4.12: Configuration 1 MEG for different distances

The results on figure 4.9 show that there are oscillations on ECC for different distances, however for the sought bandwidths (2.4-2.44 and 5.15-5.8 GHz) the value of the enveloped correlation coefficient is below 0.1, which shows a low correlation between antennas. As these parameters depend of ECC value and its value is considered low, the diversity gain (figure 4.10) is high and the multiplexing efficiency (4.11) shows a system's efficiency superior to 65% (-1.7 dB) in the 2.4-2.48 GHz and 5.15-5.85 GHz bandwidths. The MEG results show that exists a clear oscillation of values, obtaining values close to -3 dB.

Configuration 2

The second configuration is very similar to the first one, the difference lays on the orientation of the antennas, as it can be seen on figure 4.13.

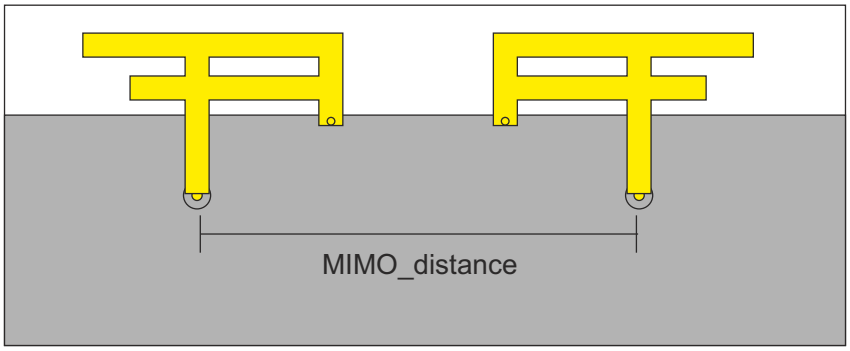

Figure 4.13: Side by side configuration 2

Figure 4.14 shows the S-parameter results. Similarly to the previous configuration, the results of each port practically match (S_{11} with S_{22} and S_{21} with S_{12}). The required bandwidths are covered.

The dependence of the antenna s-parameters on the distance between antennas is shown in figure 4.14 (S_{11}, S_{22}) and in figure 4.15 (S_{12} ,S_{21}).

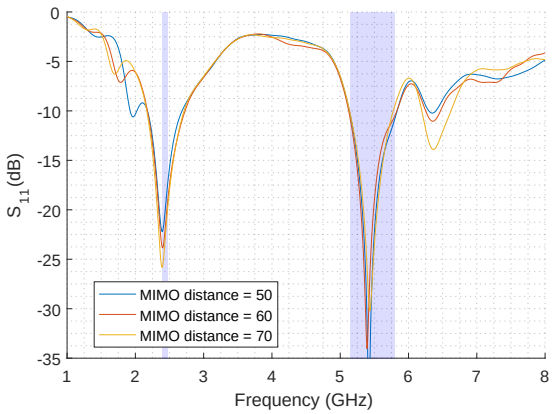

Figure 4.14: Configuration 2 distance variation S_{11} results

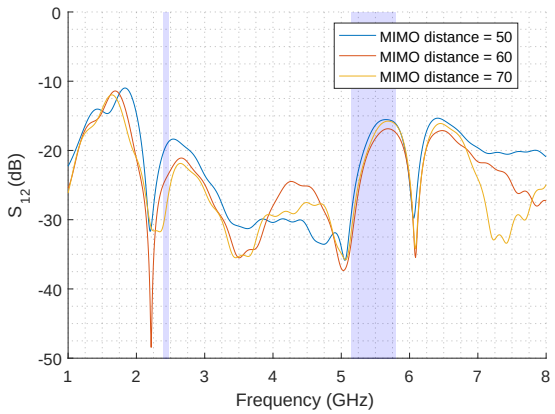

Figure 4.15: Configuration 2 distance variation S_{12} results

As for MIMO parameters results, the influence of the distance between antennas on ECC results are on figure 4.16, the DG on figure 4.17, the ME on figure 4.18 and the MEG on figure 4.19.

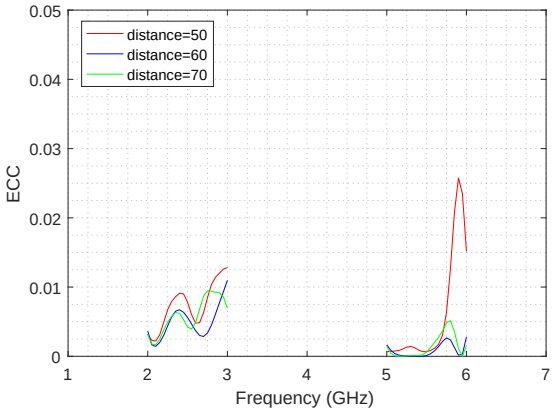

Figure 4.16: Configuration 2 ECC for different distances

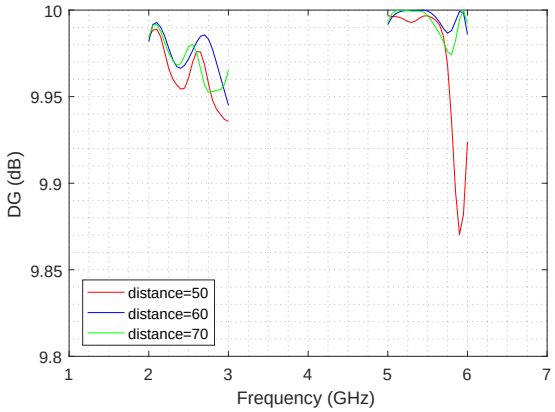

Figure 4.17: Configuration 2 DG for different distances

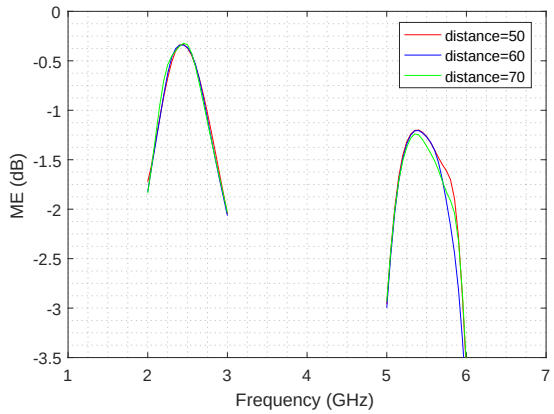

Figure 4.18: Configuration 2 ME for different distances

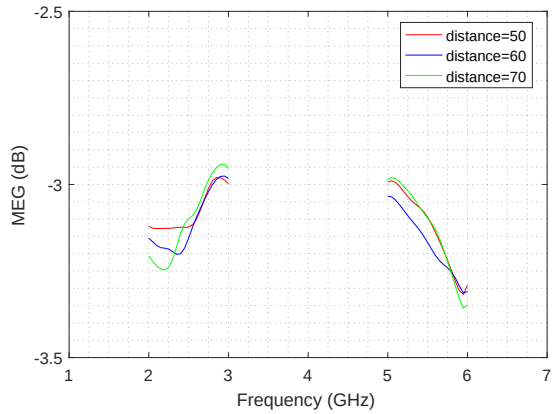

Figure 4.19: Configuration 2 MEG for different distances

The results show that the ECC value gets lower as the distance increases. The value of the enveloped correlation coefficient is below 0.01, which shows a lower correlation between the antennas of the current configuration when compared to the previous MIMO structure.

Given the results on ECC (figure 4.16), the plot observed on figure 4.17 was expected. The longer the distance between elements, the higher the DG. On the other hand, the multiplexing efficiency is almost identical for different distances.

Figure 4.19 shows the MEG results for different values of distance for port 1, which displays similar behaviour for each distance.

4.2.2 Opposite side configurations

These configurations have 2 antennas placed on the same ground plane like the previous ones, however the antennas are placed on opposite sides.

Configuration 3

The third configuration places the two antennas vertically separated by the ground plane, as it can be seen on figure 4.20.

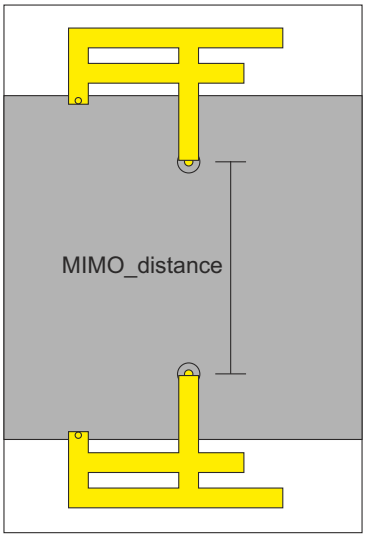

Figure 4.20: Opposite side configuration 3

As the previous configurations, the input match is simulated for different distances between antennas and the results are plotted on figures 4.21 and 4.22.

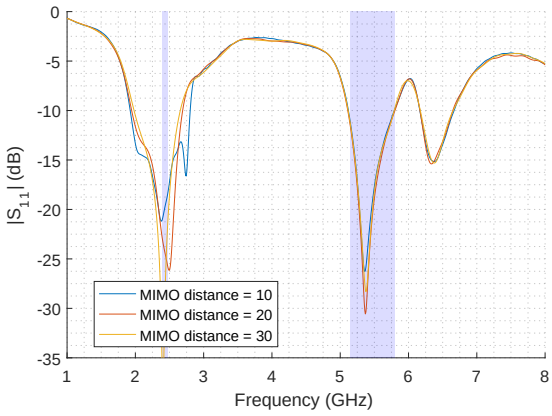

Figure 4.21: Configuration 3 distance variation S_{11} results

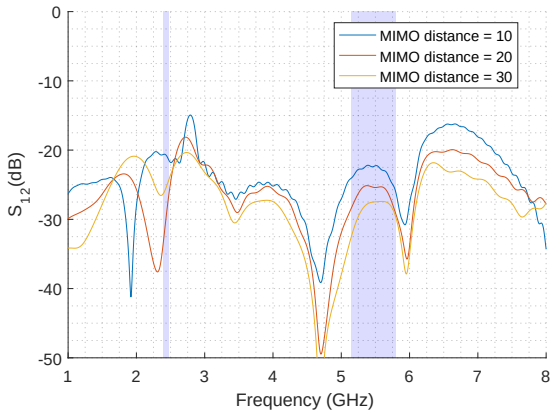

Figure 4.22: Configuration 3 distance variation S_{12} results

Analysing the results it's clear that the required bandwidth is not extended or shortened by altering the distance, however exists a better adaptation when increasing the MIMO distance, and the coupling between antennas decreases with this configuration. The ECC result is on figure 4.23, the DG is on figure 4.24. The ME and MEG are on figures 4.25 and 4.26 respectively.

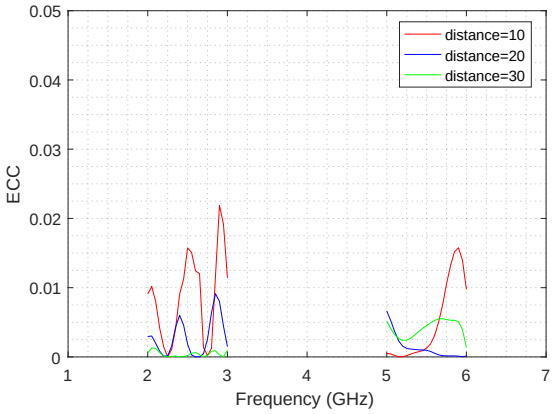

Figure 4.23: Configuration 3 ECC for different distances

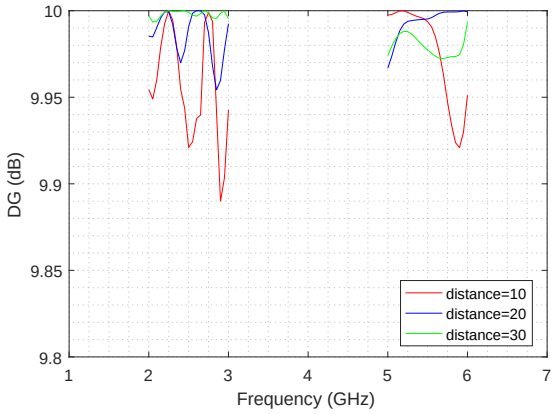

Figure 4.24: Configuration 3 DG for different distances

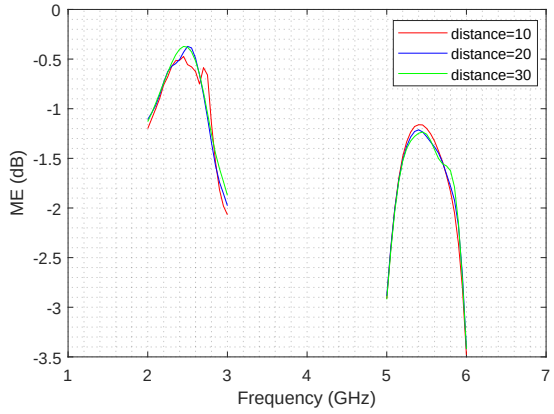

Figure 4.25: Configuration 3 ME for different distances

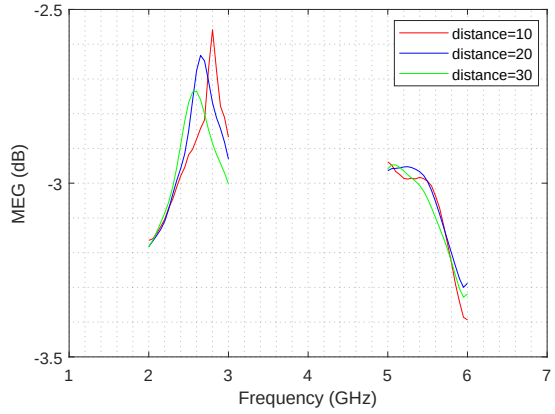

Figure 4.26: Configuration 3 MEG for different distances

With this configuration the bigger the distance between antennas, the better results are obtained; The MIMO parameter ECC shows a lower correlation when the antennas are further from each other; this makes the DG value to increase in the sought frequency bands, with gain levels in order of over 9.95 dB.

The results on figure 4.25 resemble the ones obtained in the previous structure ME after stabilizing. Examining the results on 4.26 on the determined Wi-Fi bandwidths

the MEG value increases with the distance, even though that still remains close to the -3 dB.

Configuration 4

The fourth configuration is very similar to the third one, the difference resides on the orientation of the antennas, as it can be seen on figure 4.13.

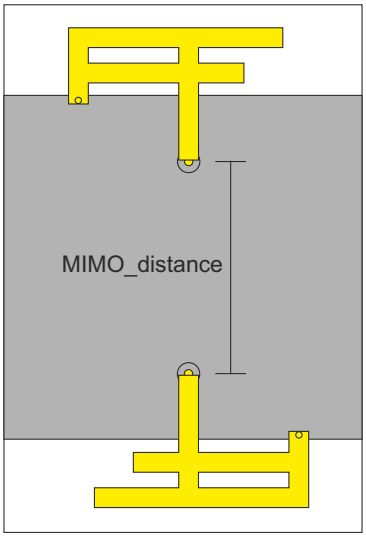

Figure 4.27: Opposite side configuration 4

As the previous configurations, the input match is simulated for different distances between antennas; the results are on figure 4.28. This plot shows an identical behaviour of the S-parameters for configuration 3 and 4, as the structures are similar. The mutual coupling is on figure 4.29.

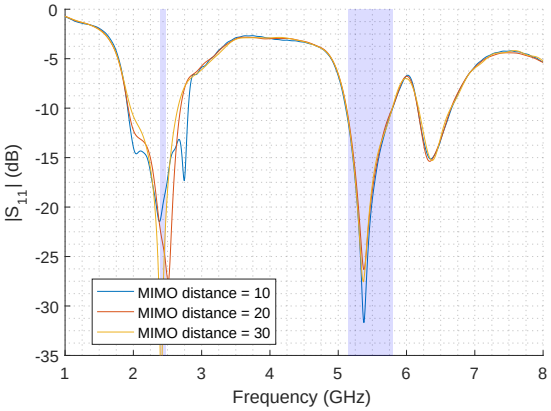

Figure 4.28: Configuration 4 distance variation S_{11} results

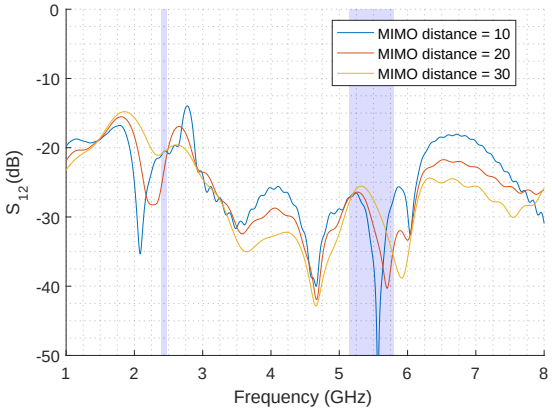

Figure 4.29: Configuration 4 distance variation S_{12} results

The ECC result is on figure 4.30 and the DG is on figure 4.31. Despite the fact that the

configurations 3 and 4 are similar and that by increasing the distance between antennas the better the performance of the system, these results show that this configuration has better results, where the ECC is a little lower and the diversity gain is closer to its theoretical maximum.

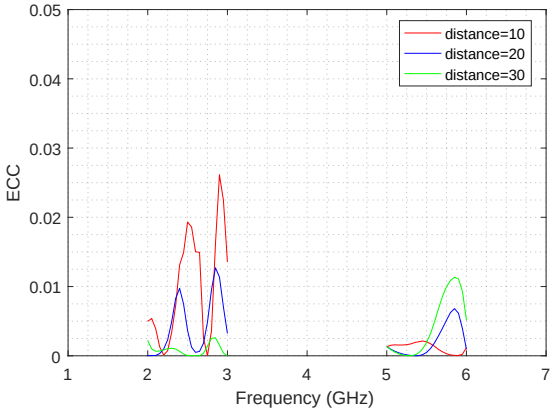

Figure 4.30: Configuration 4 ECC for different distances

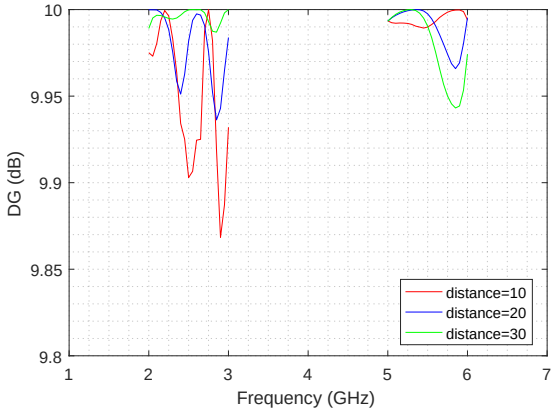

Figure 4.31: Configuration 4 DG for different distances

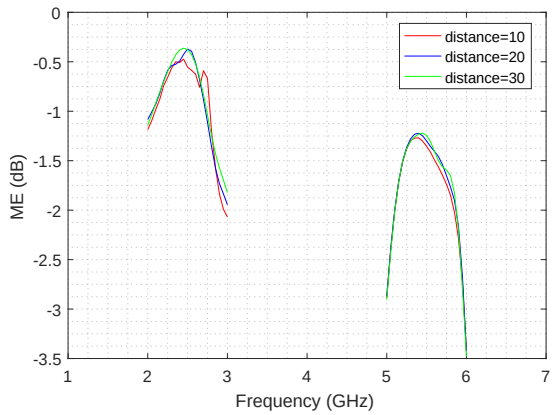

Figure 4.32: Configuration 4 ME for different distances

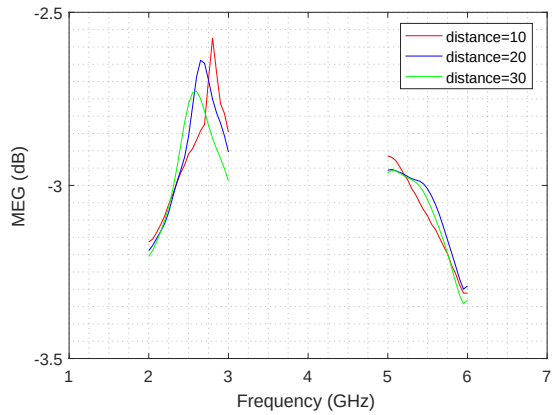

Figure 4.33: Configuration 4 MEG for different distances

Observing the figures 4.32 and 4.33, which correspond to the multiplexing efficiency and MEG results of this configuration accordingly, the results match to the previous ones; The ME has the same levels of efficiency (over 80% on 2.4 GHz band and over 70% on the 5 GHz band) and the MEG increases as the distance does it too.

4.2.3 Orthogonal configurations

These configurations have the 2 antennas placed on different adjacent sides.

Configuration 5

The fifth configuration tries to take advantage of receiving or transmitting of different angles, by placing each antenna with a different direction. The previous addition of the coaxial feeding port was to make it possible to maintain the same distance for both antennas to the design edges, as on figure 4.34.

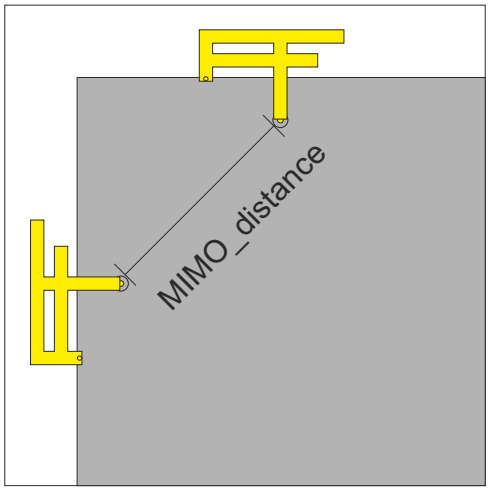

Figure 4.34: Orthogonal configuration 5

As the previous configurations, the input match is simulated for different distances between antennas; the results are on figure 4.35, that show the sought bandwidths covered and a good adaptation on it. On figure 4.36 is shown the distance dependence of the S_{12} results.

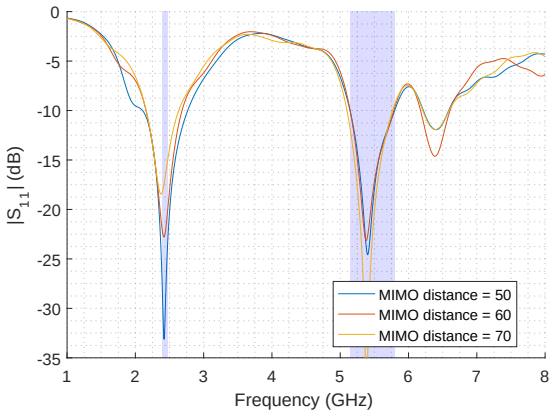

Figure 4.35: Configuration 5 distance variation S_{11} results

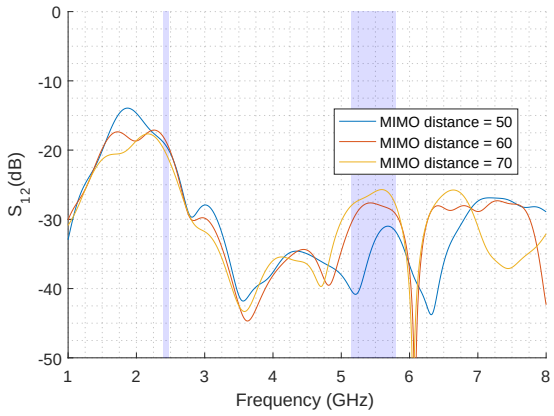

Figure 4.36: Configuration 5 distance variation S_{12} results

The ECC result is on figure 4.37, the DG is on figure 4.38 for this structure design. Although that the past configurations obtain good results in terms of MIMO parameters performance, this one takes it to another level. The results lay out a value for the correlation lower than 0.005 and a diversity gain no lower than 9.975 on the frequency bands of interest. Analysing the distance factor, just like the other tests reveal that the outcome is better as the gap between elements is widen up.

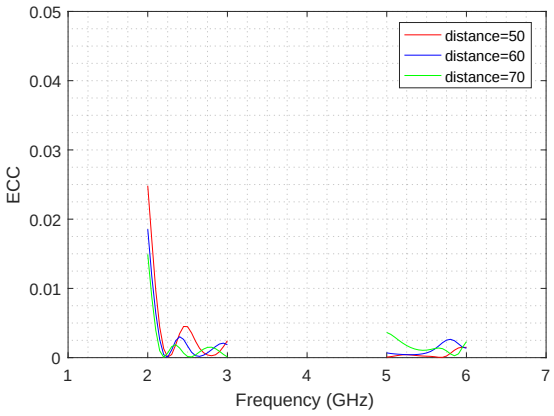

Figure 4.37: Configuration 5 ECC for different distances

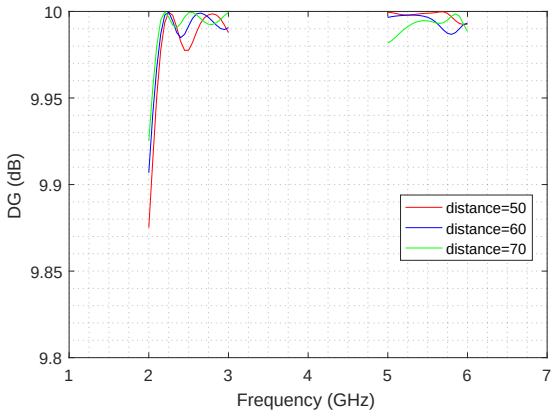

Figure 4.38: Configuration 5 DG for different distances

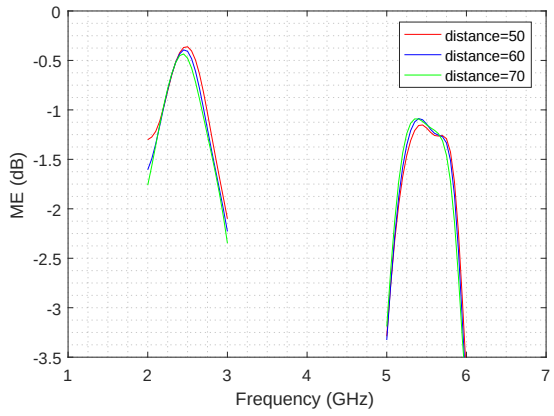

Figure 4.39: Configuration 5 ME for different distances

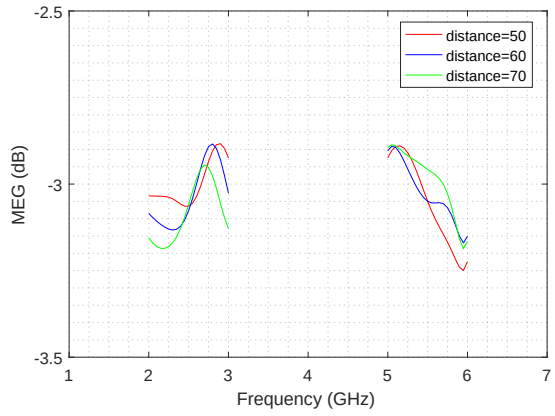

Figure 4.40: Configuration 5 MEG for different distances

Taking a look at the figures 4.39 and 4.40 the ME and MEG are presented; These parameters follow the same tendency in this design just like the earlier ones. The ME maintains the same level of efficiency on the frequency bands and the MEG is placed near the -3 dB when compared to an isotropic antenna.

Configuration 6

The sixth configuration is very similar to the fifth one, the difference resides on the orientation of the antennas, as it can be seen on figure 4.41.

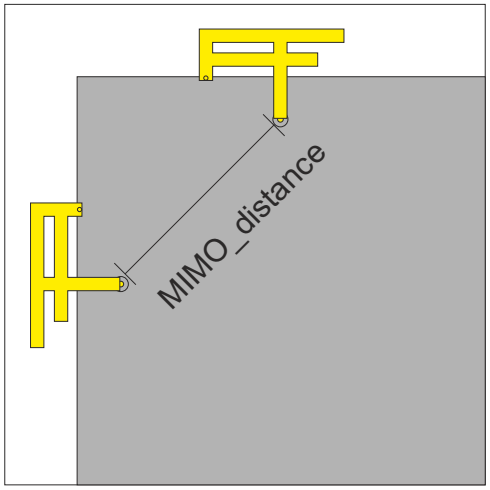

Figure 4.41: Orthogonal configuration 6

At figure 4.42 doesn't exist a notorious difference as in the anterior case, only a better matching, where increasing the distance between antennas increases the input match results.

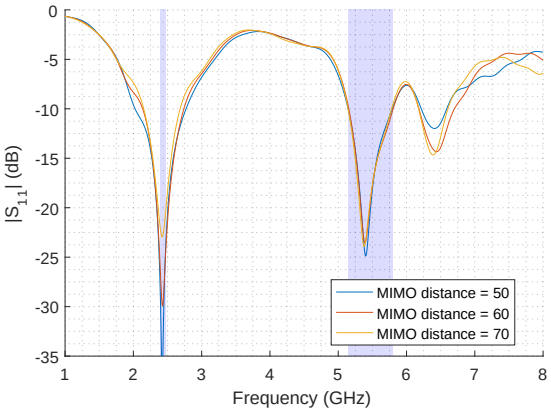

Figure 4.42: Configuration 6 distance variation S_{11} results

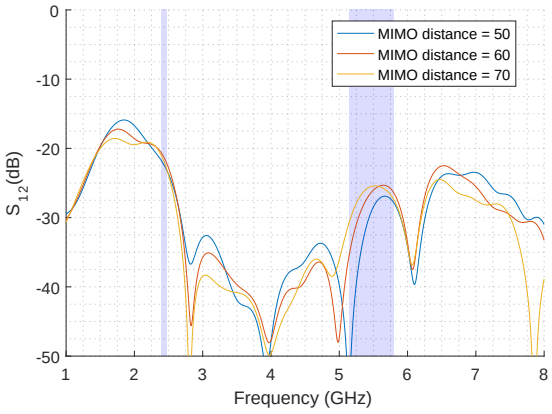

Figure 4.43: Configuration 6 distance variation S_{12} results

This configuration has similar results to the ones from configuration 5; the ECC and DG outcome are on figures 4.44 and 4.45. These plots have the same behaviour as the ones from the previous design, achieving a correlation below 0.005 between antennas and a diversity gain no lower than 9.96 dB. The wider the space between elements of the system, the better the outcome on these parameters.

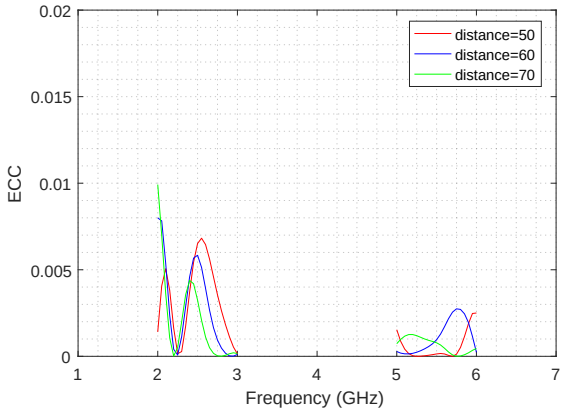

Figure 4.44: Configuration 6 ECC for different distances

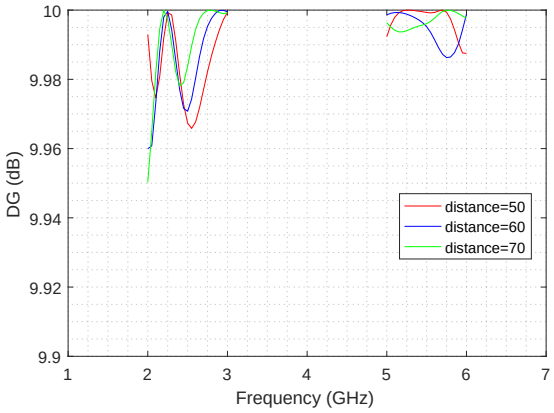

Figure 4.45: Configuration 6 DG for different distances

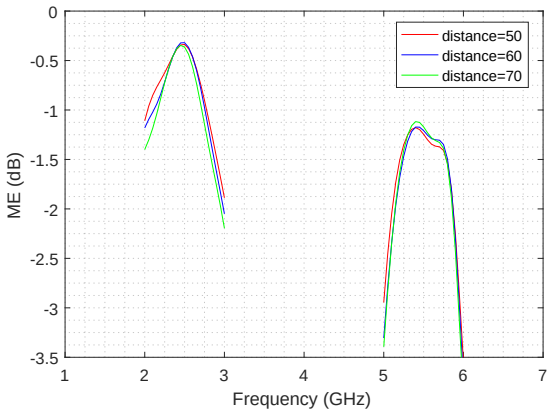

Figure 4.46: Configuration 6 ME for different distances

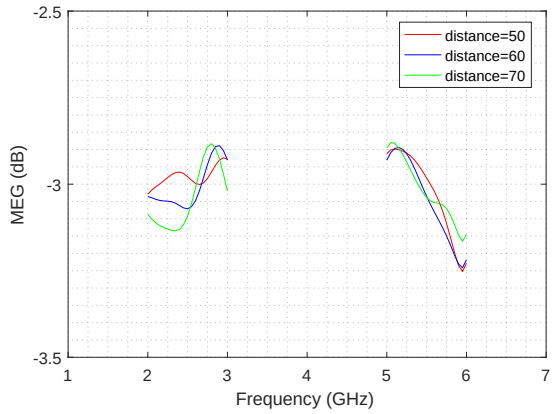

Figure 4.47: Configuration 6 MEG for different distances

For this design, the multiplexing efficiency is on figure 4.46 and the mean effective gain are on figure 4.47. The ME remains unchanged when compared to the earlier configurations, reaching efficiency superior to 70% on both frequency bands and a MEG value surrounding the -3 dB.

The main results are compiled on tables 4.2 and 4.3, the results are distinguished by the work frequency where is compared the different configurations results. Taking into account the results, the ECC values are below 0.1, which reveals that the two elements of every configuration can be considered to have a very low correlation; the diversity gain is at a high level, almost reaching the theoretical maximum (10dB); the multiplexing efficiency parameters have results of over 70% (-1.5 dB) and are directly proportional to the single antenna total efficiency. The mean effective gain is around -3

dB at every configuration, which means the MEG is reduced to half when the reference antenna is considered isotropic.

Table 4.2: Comparison between two elements configurations for 2.4 GHz

	2.44 GHz				
Configuration	S_{11}[dB]	ECC	DG [dB]	ME [dB]	MEG [dB]
conf. 1	-18.16	0.01242	9.995	-0.40	-2.97
conf. 2	-36.92	0.00621	9.997	-0.33	-3.12
conf. 3	-21.28	0.00005	9.999	-0.38	-2.83
conf. 4	-21.07	0.00033	9.998	-0.37	-2.83
conf. 5	-20.26	0.00080	9.995	-0.44	-3.01
conf. 6	-22.93	0.00422	9.979	-0.34	-3.11

Table 4.3: Comparison between two elements configurations for 5.4 GHz

	5.4 GHz				
Configuration	S_{11}[dB]	ECC	DG [dB]	ME [dB]	MEG [dB]
conf. 1	-18.55	0.00385	9.980	-1.57	-3.01
conf. 2	-18.69	0.00001	9.999	-1.24	-3.07
conf. 3	-18.33	0.00366	9.981	-1.25	-3.01
conf. 4	-23.61	0.00004	9.997	-1.23	-3.00
conf. 5	-18.38	0.00112	9.995	-1.09	-2.94
conf. 6	-17.75	0.00092	9.996	-1.12	-3.00

As shown on the previous plots, the superior band of interest (5.15 - 5.85 GHz) there exists a higher variation of the system's performance. In a more detailed analysis, it's possible to conclude that the designs that have the elements facing different directions display better results. The multiplexing efficiency results show that there is a better efficiency on the 2.4 GHz band, which follows the level of efficiencies on the single antenna design. Furthermore, adding more distance between elements improves the system performance improvement overall.

4.3 Four element MIMO antenna

The next step is to evolve to a 4-element MIMO antenna. It is chosen the configuration 5 (see figure 4.34) to use as base to the new design; its performance in terms of MIMO parameters is reliable and its design allows to make a system where all elements have the same conditions.

4.3.1 Antenna initial design

The design is presented on figure 4.48. Port 1 is associated to the top element, the other ports are distributed following the counterclockwise direction. The total dimensions of this design is 150 mm per 150 mm.

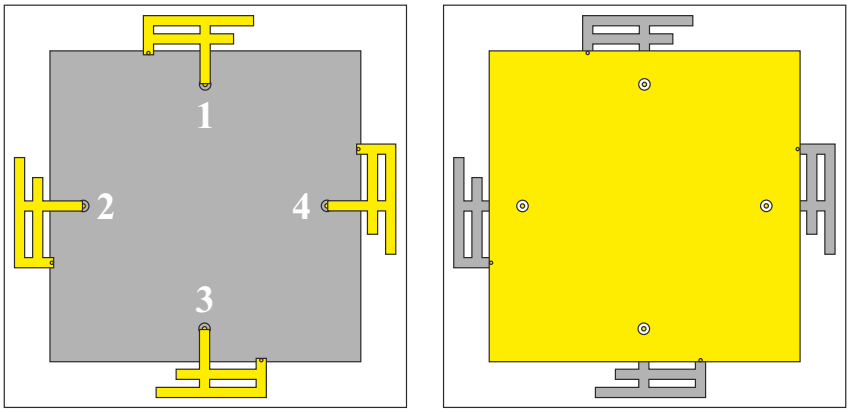

(a) front layer (b) back layer

Figure 4.48: MIMO configuration with 4 antennas

As it can be seen on figure 4.49 the required bandwidths are covered and a mutual coupling below -12 dB is achieved. The S_{12} and S_{14} results are overlapping.

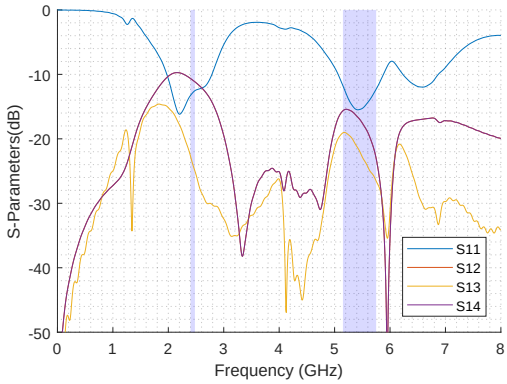

Figure 4.49: MIMO 4 antennas - port1 results

The MIMO parameters results are shown in figures 4.50, 4.51, 4.52 for port 1 and figure 4.53 shows MEG for all the configuration ports results. The remaining ports MIMO parameters show identical results due to the antenna symmetry.

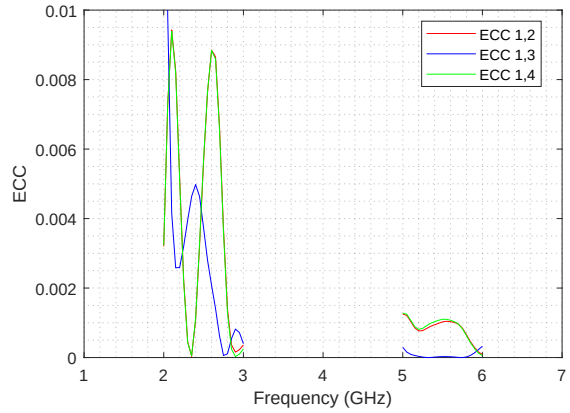

Figure 4.50: MIMO 4 antennas -ECC port1 results

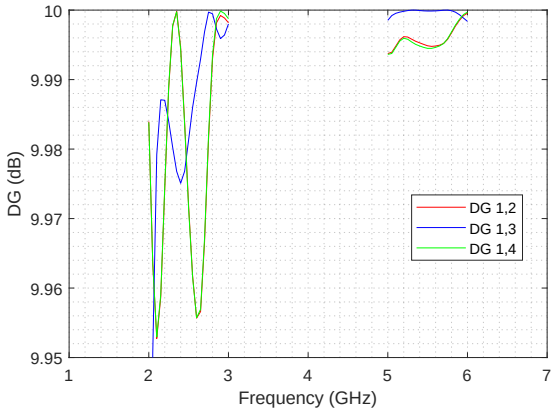

Figure 4.51: MIMO 4 antennas - DG port1 results

The ECC results demonstrate that all antennas share consonant results; Antenna 1 and 3 and the pair antenna 2-4 have coincidental results. Figure 4.51 shows a high diversity gain for the required bandwidths.

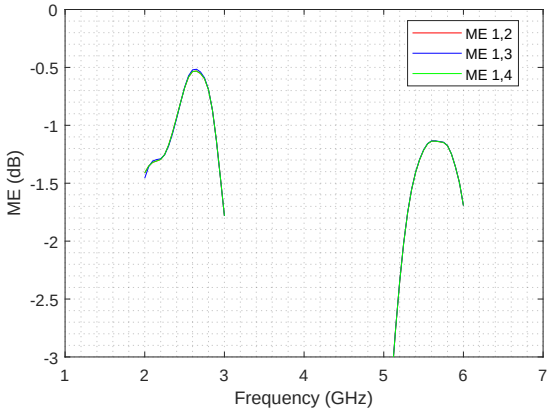

Figure 4.52: MIMO 4 antennas - ME port1 results

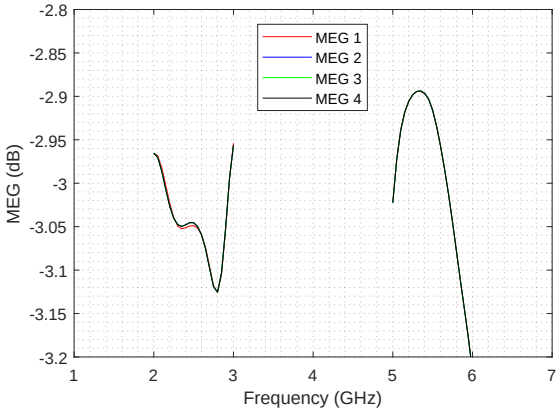

Figure 4.53: MIMO 4 antennas - MEG results

4.3.2 Antenna compact design

The previous design presents good MIMO parameters. Although this design achieves the demanded results, the size of this design is not viable for small devices. Therefore, using the same design with a few changes on the antennas dimension (which are shown on table 4.4) is presented on figure 4.54.

Table 4.4: IFA antenna dual band Parameters - 4 antennas MIMO system

Parameter	Dimension [mm]
L	28.1
L_5	8.9
W	5.3
L_{sc}	4.75
L_S	12.3

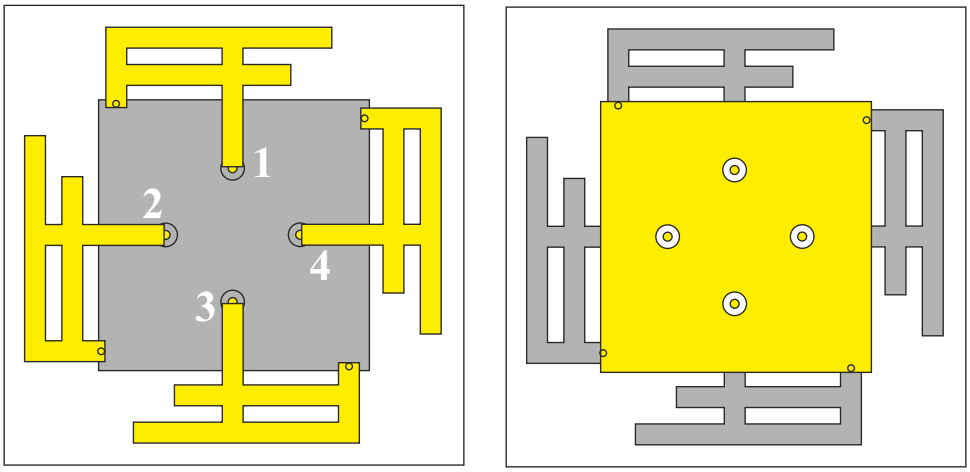

(a) front layer (b) back layer

Figure 4.54: MIMO 4 antennas - reduced design

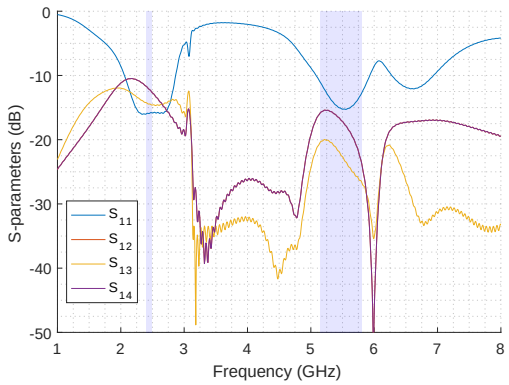

Figure 4.55: MIMO 4 antennas - port1 results

The scattering parameter results of this reduced design (see figure 4.55) are similar to the previous design and covers the required bandwidths. The S_{12} and S_{14} results are overlapping. The MIMO parameter results for port 1 are placed on figures 4.56 through 4.59.

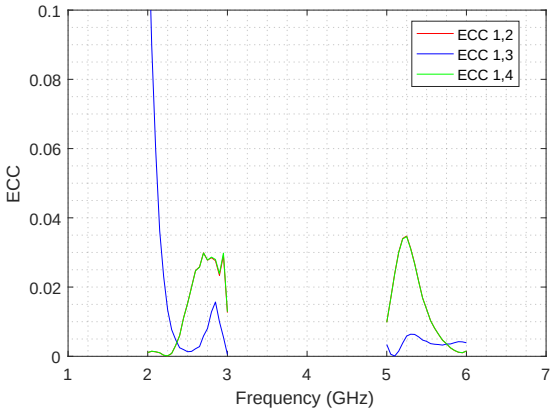

Figure 4.56: MIMO 4 antennas -ECC port1 results

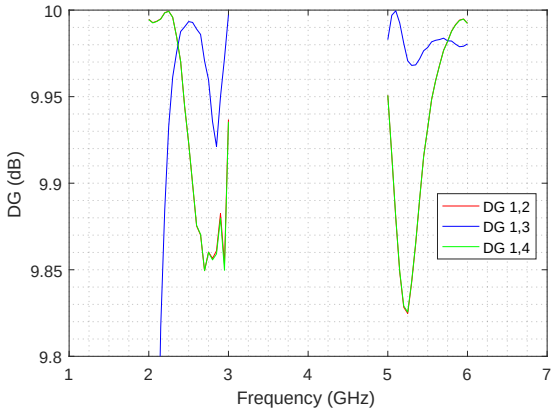

Figure 4.57: MIMO 4 antennas - DG port1 results

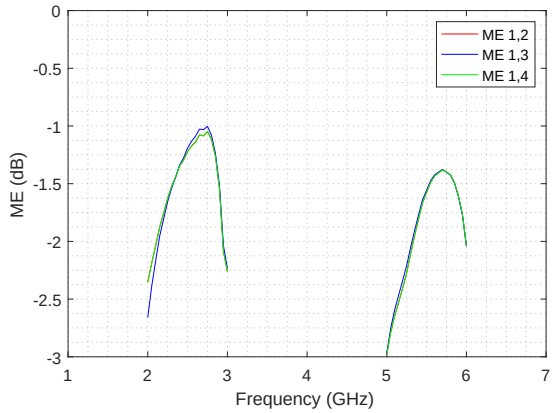

Figure 4.58: MIMO 4 antennas - ME port1 results

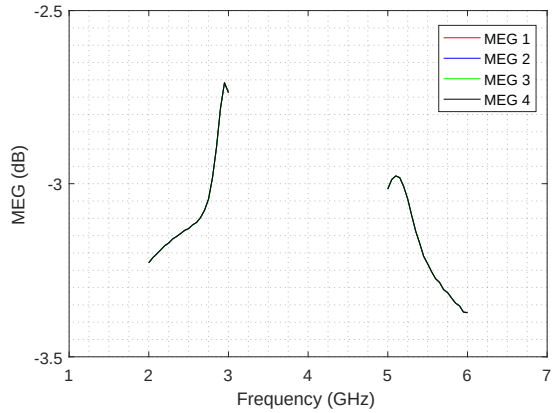

Figure 4.59: MIMO 4 antennas - MEG results

The ECC results present on figure 4.56 and the DG results on figure 4.57 behave the same way as the first 4-element system, although its results have a better performance than the current ones. This may be explained due to the dimensions reduction of the structure where it was necessary that quality-size compromise. With the current results, the ECC can achieve a level of 0.035 at the worst pairing ports, leading to a DG of 9.82 dB.

Comparing the results of the first stage 4-antenna design with the reduced design it's clear that the results are better on the previous one. However both designs have an overall acceptable results in terms of MIMO parameters. Achieving a performance-size compromise, the smaller design is chosen to be produced.

On table 4.5 a comparison of the MIMO parameters is made between the antenna of this thesis with other antennas studied. These antennas work at the same frequency

bands, although with different designs. Overall, this thesis design MIMO parameters shows a better performance than the rest of the designs.

Table 4.5: Performance comparison between different MIMO antenna designs

Reference	Frequency Band	S_{11}[dB]	ECC	DG [dB]	ME [dB]	MEG [dB]
[40]	2.4-2.48 GHz	-18	0.06	–	–	-3.7
	5.15-5.8 GHz	-18	0.013	–	–	-3.8
[41]	2.4-2.48 GHz	-16	0.01	9.5	–	–
	5.15-5.8 GHz	-41	0.2	8.6	–	–
[42]	2.4-2.48 GHz	-12	0.014	–	–	-3.7
	5.15-5.8 GHz	-12	0.125	–	–	-3.8
This work	2.4-2.48 GHz	-14.32	0.008	9.959	-1.18	-3.13
	5.15-5.8 GHz	-15.73	0.008	9.962	-1.42	-3.21

4.3.3 Prototype fabrication and measurement

The fabricated prototype is shown on figures 4.60.

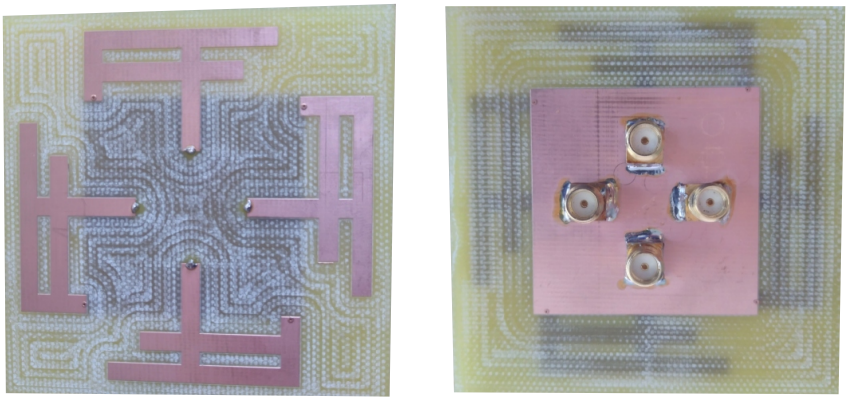

(a) front layer (b) back layer

Figure 4.60: MIMO 4 antennas prototype

The prototype performance was measured using a 4-port VNA as shown on figure 4.61.The s-parameter results of each port are on figures 4.62.

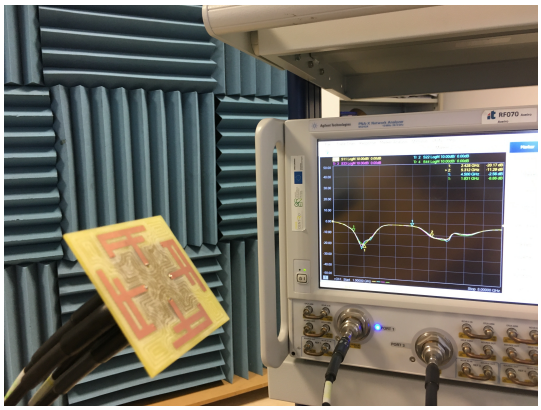

Figure 4.61: MIMO prototype measuring process

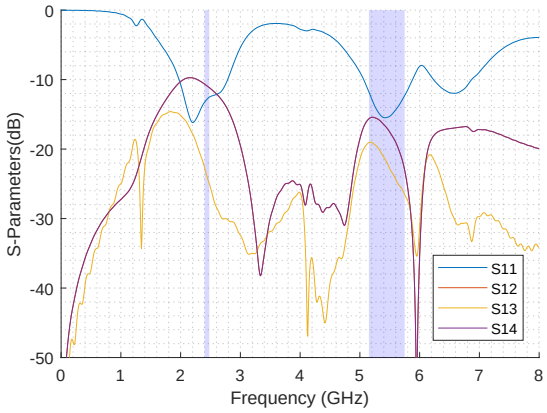

Figure 4.62: MIMO prototype measuring S-parameter results

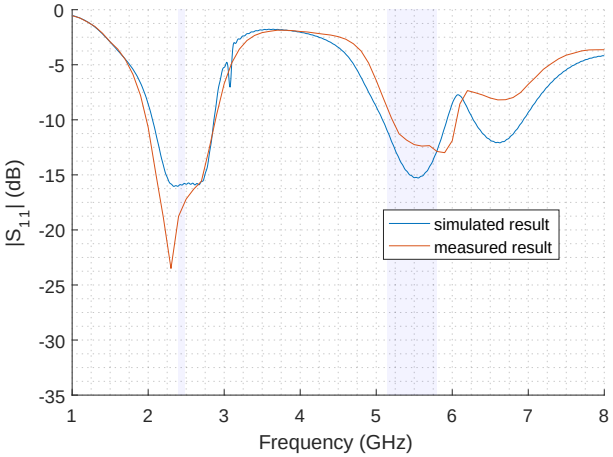

Figure 4.63: MIMO design S_{11} measured vs S_{11} simulated

In the figure 4.63 is visible that the input match are close to match, however comparing the simulated and measured outcomes there is a slight offset on the frequency bandwidth. Tables 4.6 and 4.7 show the main results from it. A good agreement between simulation and measurement is observed, which validates the antenna design.

	Bandwidth (2.4GHz)	fc [GHz]	S_{11}[dB]
Simulated	780 MHz (31.71%)	2.46	-16.22
Measured	870 MHz (35.66%)	2.47	-17.92

Table 4.6: Summary results of the prototype MIMO antenna for 2.4 GHz

	Bandwidth (5.4GHz)	fc [GHz]	S_{11}[dB]
Simulated	830 MHz (15.09%)	5.5	-15.31
Measured	930 MHz (16.32%)	5.7	-12.53

Table 4.7: Summary results of the prototype MIMO antenna for 5.4 GHz

5

Conclusions

This chapter presents a summary of all the work presented in this thesis, revisiting the main conclusions that were obtained. Also, some possible tasks for a future work are given.

5.1 Conclusions

The purpose of this thesis MSc dissertation was to design an antenna that could cover the Wi-Fi Bandwidths (2.4 and 5 GHz) and elaborate a MIMO system based on it. This dissertation also presents the study of MIMO parameters of different MIMO configurations, with focus on space diversity influence.

The design process was described in the previous chapters, which include the simulated results of each stage. The proposed antenna is a planar IFA; this design proved to be a good choice, as it allowed to reach this project's goals with a good performance, due to its tunable dimensions to define each work frequency and a relative small size.

In this project different 2 antenna MIMO configurations with the IFA design as the systems' antennas was studied, where the return loss, coupling of the antennas and the relevant MIMO parameters were measured: diversity gain, envelope correlation coefficient, multiplexing efficiency and mean effective gain. The results show that every MIMO configuration obtains satisfactory values for each parameter; and the simulations support that increasing the distance between the antennas (raising the space diversity) improves the MIMO parameters' results. One of these configurations was extended to a 4 antenna MIMO system.

Analysing the case of each MIMO parameter, the correlation coefficient is lower as the distance between antennas increase, leading to increase of the theoretical diversity gain. It's also notable that the multiplexing efficiency doesn't have a strong dependence on the distance between elements. The mean effective gain results take up values close to the -3 dB, which means that this thesis design has approximately half the mean effective gain of a isotropic antenna.

A prototype of the IFA antenna design was fabricated, and its input match was measured; the results don't exactly match the simulated results and could not cover all the bandwidth required. Even with the slight offset, the prototype results follow the design's simulation outcome.

A 4 antenna MIMO system prototype was also created and measured. The S-parameter results demonstrate a similar behaviour to the anticipated. Although there is some requisite frequency band not covered, the results show that this MIMO system geometry is viable for both WiFi bands application.

5.2 Future Work

Although this dissertation's goal was achieved, there are some aspects that can be improved, which could optimize the final antenna system; these aspects include:

- Use a more stable substrate material instead of the current one (FR4) on the antenna's manufacturing;
- Improve the reference IFA design, in order to acquire a larger bandwidth margin, and trying to reduce the design's size;
- Measure and study the radiation patterns of the prototype antenna, and make the comparison with the simulated one;
- Measuring the MIMO structures prototype at a controlled environment in order to compare with the reference design simulations and its MIMO parameters results;
- Evaluate the performance of the manufactured antenna system in a router environment (e.g. placing the MIMO system on a plastic case in the presence of other electronic components).

Bibliography

[1] E. Notes, "Wifi frequency bands list," accessed in january 2020. https://www.electronics-notes.com/articles/connectivity/wifi-ieee-802-11/channels-frequencies-bands-bandwidth.php/.

[2] E. Notes, "Mimo formats - siso, simo, miso, mimo," accessed in january 2020. https://www.electronics-notes.com/articles/antennas-propagation/mimo/siso-simo-miso-mimo.php.

[3] A. J. Paulraj, D. A. Gore, R. U. Nabar, and A. Bolcskei, "An overview of mimo communications — a key to gigabit wireless," IEEE wireless communications, pp. 1–4, 2016.

[4] J. Yuan, Q. He, M. Matthaiou, T. Q. S. Quek, and S. Jin, "Toward massive connectivity for iot in mixed-adc distributed massive mimo," IEEE Internet of Things Journal, vol. 7, pp. 1841 – 1856, 2019.

[5] "Mimo formats," accessed in november 2019. https://www.rfwireless-world.com/Terminology/MIMO.html.

[6] A. Goldsmith, S. A. Jafar, N. Jindal, and S. Vishwanath, "Capacity limits of mimo channels," IEEE J. Select Areas Commun, vol. 21, pp. 684–702, 2003.

[7] I. Stevanovic, A. Skrivervik, and J. R. Mosig, "Smart antenna systems for mobile communications," tech. rep., Ecole Polytechnique Fédérale de Lausanne, 2003.

[8] H. Ramezani, "Mimo rayleigh fading channel capacity," accessed in april 2018. https://www.mathworks.com/matlabcentral/fileexchange/12491-mimo-rayleigh-fading-channel-capacity.

[9] C. W. Deshun Sun, "Analysis and design of 4 × 4 mimo-antenna systems in mobile phone," Journal of Computer and Communications, pp. 26–33, 2016.

[10] J. R. S. Blanch and I. Corbella, "Exact representation of antenna system diversity performance from input parameter description," Electronics Letters Online, vol. 39, pp. 705–707, 2003.

[11] M. Koohestani, H. Ahmed, A. A. Moreira, and S. K. Anja, "Diversity gain influenced by polarization and spatial diversity techniques in ultrawideband," IEEE wireless communications, pp. 1–3, 2015.

[12] a. Z. Y. Ruiyuan Tian, Buon Kiong Lau, "Multiplexing efficiency of mimo antennas with user effects," Proceedings of the 2012 IEEE International Symposium on Antennas and Propagation, 8-14 July 2012, Chicago, IL, USA.

[13] a. Z. Y. Ruiyuan Tian, Buon Kiong Lau, "Multiplexing efficiency of mimo antennas," IEEE Antennas and Wireless Propagation Letters, vol. 10, pp. 183–186, 2011.

[14] F. T. A. Alayón Glazunov, A.F. Molisch, "Mean effective gain of antennas in a wireless channel," IET Microwaves, Antennas & Propagation, vol. 3, pp. 214–227, 2009.

[15] T. Taga, "Analysis for mean effective gain of mobile antennas in land mobile radio environments," IEEE Transactions on Vehicular Technology, vol. 39, pp. 117 – 131, 1990.

[16] S.-Y. H. Wen-Jiao Liao, Te-Ming Liu, "Miniaturized pifa antenna for 2.4 ghz ism band applications," 6th European Conference on Antennas and Propagation (EUCAP), 26-30 March 2012, Prague, Czech Republic.

[17] J. Saini and S. K. Agarwal, "Design a single band microstrip patch antenna at 60 ghz millimeter wave for 5g application," 2017 International Conference on Computer, Communications and Electronics (Comptelix), 1-2 July 2017, Jaipur.

[18] M. M. T. F. N. M. Redzwan, M.T. Ali and N. Miswadi, "Design of planar inverted f antenna for lte mobile phone application," IEEE Region 10 Symposium, 14-16 April 2014, Kuala Lumpur, Malaysia.

[19] L.-H. Wen, S. Gao, Q. Luo, C.-X. Mao, W. Hu, Y. Yin, Y. Zhou, and Q. Wang, "Compact dual-polarized shared-dipole antennas for base station applications," IEEE Transactions on Antennas and Propagation, vol. 66, pp. 6826 – 6834, 2018.

[20] N. Chang and J.-H. Jiang, "Meandered t-shaped monopole antenna," IEEE Transactions on Antennas and Propagation, vol. 57, pp. 3976–3978, 2009.

[21] S.-H. Yeh and K.-L. Wong, "Integrated f-shaped monopole antenna for 2.4/5.2 ghz dual-band operation," Microwave and Optical Technology Letters, vol. 34, pp. 24–26, 2002.

[22] J. Qi Luo and H.M.Salgado, "Fractal monopole antenna for wlan usb dongle," Loughborough Antennas & Propagation Conference, 16-17 November 2009, Loughborough, UK.

[23] M. Ye, Y. Zhang, C. Wu, J. Cheng, and Z. Liu, "Dual-band inverted-f antenna with tunable inductor and capacitor for 5g mobile communication," International Conference on Integrated Circuits, Technologies and Applications, 21-23 November 2018, Beijing, China.

[24] M. A. Osama M. Haraz and S. Alshebeili, "Single-band pifa mimo antenna system design for future 5g wireless communication applications," International Conference on Wireless and Mobile Computing, Networking and Communications (WiMob), 2015.

[25] Y.-C. L. Yu-Kai Tseng and L.-T. Hwang, "Implementation of a mimo antenna design for usb dongle applications," Electronic Components & Technology Conference, 28-31 May 2013, Las Vegas, NV, USA.

[26] J. Qi Luo, Chris Quigley and H.M.Salgado, "Inverted-l antennas array in a wireless usb dongle for mimo application," European Conference on Antennas and Propagation (EUCAP), 26-30 March 2012, Prague, Czech Republic.

[27] S. E. Maddur and Y. Gurramkonda, "T slit koch fractal compact mimo antenna with high isolation and polarization diversity," Second International Conference on Electronics, Communication and Aerospace Technology (ICECA), 29-31 March 2018, Coimbatore, India.

[28] Q. Luo, H.M.Salgado, and J.R.Pereira, "Compact printed monopole antenna array for dualband wlan application," IEEE Antennas and Wireless Propagation Letters, 27-29 April 2011, Lisbon, Portugal.

[29] O. M. H. Mohamed Mamdouh M. Ali, Andrew M. Azmy, "Design and implementation of reconfigurable quad-band microstrip antenna for mimo wireless communication applications," National Radio Science Conference (NRSC2014), 28-30 April 2014, Cairo, Egypt.

[30] H. Li and B. K. Lau, "Design of low profile mimo antennas for mobile handset using characteristic mode theory," IEEE 5th Asia-Pacific Conference on Antennas and Propagation (APCAP), 26-29 July 2016, Kaohsiung, Taiwan.

[31] K. T. S. S. Rajkumar and P. H. Rao, "Compact two-element uwb fractal monopole mimo antenna using t- shaped reflecting stub for high isolation," IEEE International Microwave and RF Conference (IMaRC), 10-12 December 2015, Hyderabad, India.

[32] W. Hu, L. Qian, S. Gao, L.-H. Wen, Q. Luo, H. Xu, X.-K. Liu, Y. Liu, and W. Wang, "Dual-band eight-element mimo array using multi-slot decoupling technique for 5g terminals," IEEE Access, vol. 7, pp. 153910 – 153920, 2019.

[33] D. S. Xuanxuan Wang, Wenxiu Wang and Y. Gao, "Design and simulation of td-lte dual-mode mobile terminal antenna combined with mimo technology," 6th Asia-Pacific Conference on Environmental Electromagnetics (CEEM), 6-9 November 2012, Shanghai, China.

[34] A. Peristerianos, A. Theopoulos, A. G. Koutinos, T. Kaifas, and K. Siakavara, "Dual-band fractal semi-printed element antenna arrays for mimo applications," IEEE Antennas and Wireless Propagation Letters, vol. 15, pp. 730 – 733, 2015.

[35] T. S. Deukhyeon GA, Younggi Lee and J. Choi, "Design of mimo antenna with decoupling network for lte mobile application," Asia Pacific Microwave Conference Proceedings, 4-7 December 2012, Kaohsiung, Taiwan.

[36] S. Padmanathan, A. A. Al-Hadi, P. J. Soh, and M. F. Jamlos, "Dual port mimo half-shaped cubical parasitic pifa design for pattern and frequency reconfiguration applied in mobile terminals," Asia-Pacific Conference on Applied Electromagnetics (APACE), 11-13 December 2016, Langkawi.

[37] M. Peng, H. Zou, Y. Li, M. Wang, and G. Yang, "An eight-port 5g/wlan mimo antenna array with hexa-band operation for mobile handsets," International Symposium on Antennas and Propagation & USNC/URSI National Radio Science Meeting, 8-13 July 2018, Boston, MA, USA.

[38] I.T.E.Elfergani, A. S. Hussaini, R. Abd-Alhameed, C.H.See, M.B.Child, and J. Rodriguez, "Design of a compact tuned antenna system for mobile mimo applications," Loughborough Antennas & Propagation Conference (LAPC), 12-13 November 2012, Loughborough, UK.

[39] T. S. P. S. Zhi Ning Chen, Xianming Qing and W. K. Toh, "Antennas for wifi connectivity," Proceedings of the IEEE, vol. 100, pp. 2322–2329, 2012.

[40] S. Soltani, P. Lotfi, and R. D. Murch, "A port and frequency reconfigurable mimo slot antenna for wlan applications," IEEE Transactions on Antennas and Propagation, vol. 64, pp. 1209 – 1217, 2016.

[41] A. D. C. L. Rafik Addaci, Katsuyuki Haneda and P. Vainikainen, "Dual-band wlan multiantenna system and diversity/mimo performance evaluation," IEEE Transmission Antennas Propagation, vol. 62, p. 1409–1415, 2014.

[42] S. Soltani, P. Lotfi, and R. D. Murch, "A dual-band multiport mimo slot antenna for wlan applications," IEEE Antennas and Wireless Propagation Letters, vol. 16, pp. 529 – 532, 2016.

[43] C. A. Balanis, Antenna Theory Analysis and Design. Wiley, 2009.